Interference Suppression for Spread Spectrum Signals Using Adaptive Beamforming and Adaptive Temporal Filter

THESIS

Wonjin Park
Captain, Republic of Korea Army

AFIT/GE/ENG/96D-14

DEPARTMENT OF THE AIR FORCE
AIR UNIVERSITY
AIR FORCE INSTITUTE OF TECHNOLOGY

Wright-Patterson Air Force Base, Ohio

AFIT/GE/ENG/96D-14

Interference Suppression for Spread Spectrum Signals Using Adaptive Beamforming and Adaptive Temporal Filter

THESIS

Wonjin Park
Captain, Republic of Korea Army

AFIT/GE/ENG/96D-14

The views expressed in this thesis are those of the author and do not reflect the official policy or position of the Department of Defense or the U. S. Government.

AFIT/GE/ENG/96D-14

Interference Suppression for Spread Spectrum Signals Using Adaptive Beamforming and Adaptive Temporal Filter

THESIS

Presented to the Faculty of the School of Engineering

of the Air Force Institute of Technology

Air University

In Partial Fulfillment of the

Requirements for the Degree of

Master of Science in Electrical Engineering

Wonjin Park, B.S.E.E

Captain, Republic of Korea Army

December, 1996

Acknowledgements

There are many people to thank for their patience, support and knowledge. Without them this thesis would not have been in birth.

Foremost, to my wife, KyungRan, thank you your love, support, and hard work over the last 30 months with me. I would like to thank my advisor, Major Gerald Gerace, for his guidance and motivation throughout this research effort. I would also like to thank all of my senior officers, especially Capt Hyunki Cho, for providing me with the support, encouragement and help with the computer problems I experienced. Finally, to the Republic Korean Army for affording me this great opportunity.

Wonjin Park

Table of Contents

List of Figures

List of Tables

Abstract

Interference and jamming signals are a serious concern in an operational military communication environment. This thesis examines the utility and performance of combining adaptive temporal filtering with adaptive spatial filtering (i.e. adaptive beamforming) to improve the signal-to-jammer ratio (SJR) in the presence of narrowband and wideband interference. Adaptive temporal filters are used for narrowband interference suppression while adaptive beamforming is used to suppress wideband interference signals. A procedure is presented for the design and implementation of a linear constraints minimum variance generalized sidelobe canceler (LCMV-GSC) beamformer. The adaptive beamformer processes the desired signal with unity gain while simultaneously and adaptively minimizing the output due to any undesired signal. Using the LCMV-GSC beamformer with a least mean squares (LMS) adaptive algorithm, it was shown that the tapped delay line (TDL) adaptive antenna array is more effective for the suppression of wideband jammer suppression than the linear array sensors (LAS) adaptive antenna array. Also a new technique for adaptive beamforming is presented which improves wideband interference suppression in a frequency-hopped environment. The output SJR improvement for the new technique compared to the conventional technique is as much as 15dB. Sometimes, multipath signals and jammers generated by a smart enemy are correlated with the desired signal which destroys the traditional beamformer's performance. After performing a spatial smoothing technique, adaptive beamforming can also be effective in suppressing the jamming signals that are highly correlated with the desired signal.

Interference Suppression for Spread Spectrum Signals Using Adaptive Beamforming and Adaptive Temporal Filter

I. Introduction

1.1 Background

The final goal of communication is to transmit information without error from a transmitter to a receiver. In the real world, there are several interference sources with various powers and bandwidths to prevent this goal. These interfering signals might arise from intentional jamming, multipath, multiple users on the same bandwidth, or a variety of other sources. In a noisy, crowded, or hostile environment, a number of techniques may be implemented in order to increase the anti-jam characteristics of a communication system. Some methods include spread spectrum modulation, interference suppression and spatial discrimination techniques.

The objective of this research is to examine the effectiveness of adaptive algorithms for interference suppression in spread spectrum communication. It is desirable to achieve temporal and spatial filtering using adaptive algorithms to maintain an acceptable signal-to-noise ratio (and hence, probability of bit error) in any kind of interference such as intentional jamming, multipath, and co-channel interference.

1.1.1 Spread Spectrum Modulation. Spread Spectrum techniques have an inherent ability to suppress interference (Peterson at el, 1995). These are modulation schemes that produce a spectrum with a much wider bandwidth than that of the information bearing signal. By increasing the bandwidth over which signal energy is contained, the energy density of the signal is reduced and hidden in the noise levels so that unintended receivers cannot detect it. Hence the signals have a low probability of intercept. Upon reception of the desired signal and undesired jammer signal by the Spread Spectrum (SS) receiver, the coding process is reversed and the signal energy density

is returned to its original level while the jammer energy density is reduced. Hence the receiver is resistant to interference and jamming.

Two common spread spectrum schemes are direct sequence (DS) and frequency hopping (FH). Direct Sequence is achieved by combining a binary message sequence and a higher rate pseudorandom binary sequence. A pseudorandom binary sequence code has a much higher rate than the original digital data which expands the bandwidth beyond that of the original information bandwidth. Frequency hopping is achieved by changing the frequency of the carrier periodically. Typically, each carrier frequency is chosen from a set of 2^k frequencies which are spaced apart approximately the width of the data modulation bandwidth. The frequency is translated to one of 2^k frequency hop bands by the FH modulator. The processing gain is 2^k. The spreading code in this case does not directly modulate the carrier but is instead used to control the sequence of carrier frequencies.

1.1.2 Interference Suppression. The inherent processing gain of a spread spectrum signal will, in many case, provide the system with a sufficient degree of interference rejection capability. However, if the combined interference signal power relative to the desired signal power exceeds the spread spectrum processing gain, additional filtering is required. If the interference is relatively narrowband compared with the bandwidth of the spread spectrum, then interference suppression by the use of notch filters often results in an improvement in system performance.

There are two techniques for building notch filters. The first technique uses a transversal filter in the time domain (Milstain and Das, 1980; Saulnier, 1990). The system can be made adaptive by using a tapped delay line with variable tap weights. These tap weights can be adapted, for example, by using the well-known least-mean-square (LMS) algorithm.

The second technique is that of transform domain processing. A notch filter is implemented by Fourier transforming the received waveform, applying some type of signal processing algorithm, and then inverse Fourier transforming the signal back to the time domain. One type of signal

processing algorithm excises the frequency bin which exceeds a specific threshold (Milstain and Das, 1980). Another way is to use adaptive transform domain filtering (Saulnier, 1992). This type of suppressor combines features of the time domain adaptive filter and the transform domain excisor. The transform domain technique works more effectively than the time domain technique for all interference bandwidth. Transform domain techniques are also more robust since they can handle multiple narrowband jammers simultaneously.

1.1.3 Spatial Discrimination Technique. Spatial discrimination techniques include adaptive null steering antennas and high-gain directional antennas (Widrow et al, 1982). Together, they place nulls of the receiver's antenna pattern in the direction of enemy jammers to avoid front end saturation of the receiver and to increase the gain in the direction of the desired signal. In an adaptive array, the phase and amplitude of the signal at each receiving antenna element is weighted and the resulting signals summed to produce the array output. The values of the element weights are determined by an algorithm that can act to steer nulls in the direction of interfering signals (Fig. 1.1).

1.2 Problem Statement and Objective

Any kind of interference signals are a serious concern in an operational military communication environment. Many researchers have developed lots of techniques for narrowband interference suppression, i.e. adaptive filter in time and transform domain and excisor. In the case of wideband interferences, those techniques can't work, because the desired signal is also suppressed when they suppress the wideband interferences. Until now, the adaptive beamforming is known as the way to suppress the wideband interferences. However, the wideband interferences suppression remains an important research topic. Furthermore, multipath signals are correlated to the desired signal and the smart jammer uses the correlated signal with the desired signal to prevent our communication.

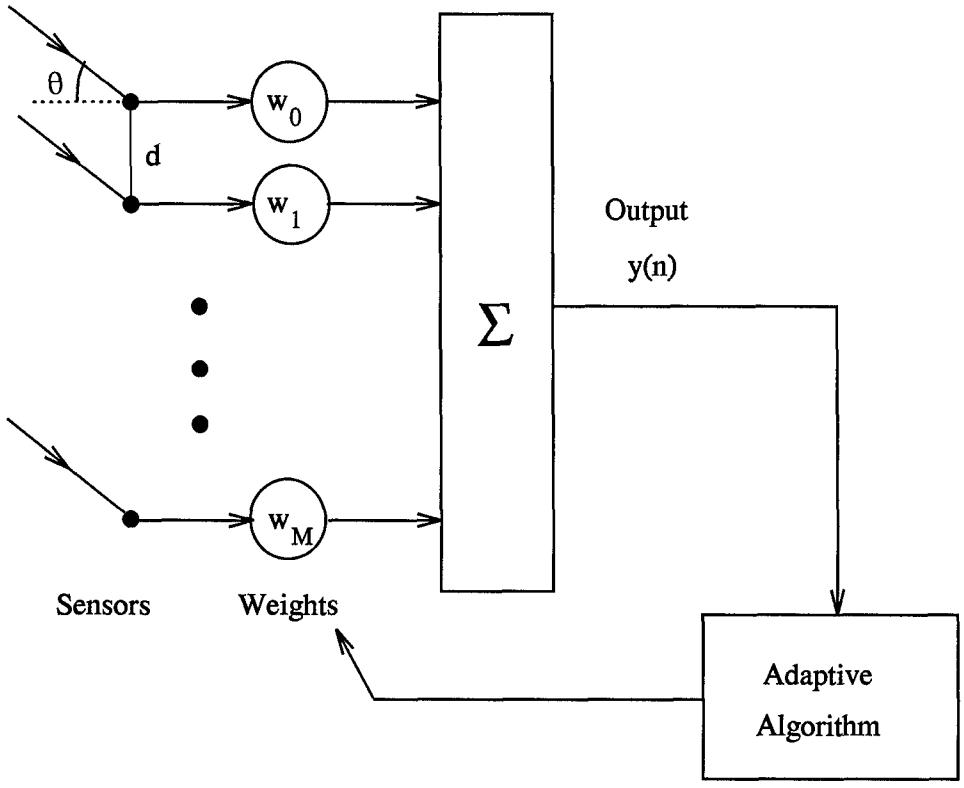

Figure 1.1 Linear Antenna Array for Spatial Processing

The conventional adaptive beamforming is totally destroyed in the presence of correlated signals. The correlated interference is a serious problem in the traditional adaptive beamformer.

This research combines a notch filter technique and spatial discrimination technique which are two of the most powerful methods for providing interference signal suppression. In other words, by achieving adaptive temporal and spatial filtering using adaptive algorithm, the system maintains the reasonable signal power to jammer power ratio (SJR).

1.3 Assumption

The research assumes that the received signal is composed of a sum of jamming and desired signals. It is also assumed that code synchronization is maintained at the communication receiver, and thus, there is no propagation delay. Finally, unless explicitly mentioned, the desired signal and jamming signal are uncorrelated each other. The antenna elements are uniformly distributed and

the distance between elements is a half wavelength of the desired signal center frequency in order to prevent the grating lobe. Those assumptions are reasonable for real situation and hardware, thus they doesn't affect the result of simulation.

1.4 Scope

The desired signal considered in this research has wide bandwidth. Specifically, frequency hopped signals are considered because FH (Frequency Hopping) signals and antenna arrays are closely related. Each antenna element is omni-directional. Jammer models consist of both narrow and wide bandwidth. The adaptive algorithm used in both schemes is the LMS (Least Mean Squares) algorithm. This algorithm is the best known and most easily implemented algorithm which implement an iterative solution to the Wiener-Hoff equation without making use of any a priori statistical information about the received signal. The Wiener-Hoff equation determines the optimal tap weight settings for the transversal filter.

The class of adaptive beamformer discussed is LCMV-LMS (Linearly Constrained Minimum Variance - Least Mean Squares) beamforming which constrains the gain and phase in the desired signal direction and minimizes the output due to the undesired signals (Griffiths and Jim, 1982). For LCMV beamforming, a GSC (Generalized Side-lobe Canceller) structure is used because this structure is useful for implementation and analysis of LCMV beamforming.

1.5 Material and Equipment

All system models and simulations were developed using the version 4.1 Matlab simulation software developed by The Math Works, Natric, Massachusetts. The software was run on a Sun Workstation.

1.6 Thesis Organization

Chapter II of this thesis highlights a literature review of adaptive algorithm, adaptive beamforming, and adaptive signal processing in spread spectrum modulation. Chapter III presents a basic introduction into the concept of adaptive signal processing. It compares the temporal filter versus spatial filter. It then discusses the theory of adaptive temporal filters and adaptive beamforming. Moreover, the adaptive beamforming in the presence of correlated signals is presented. Chapter IV provides the simulation results related to jamming suppression and especially emphasizes the jamming suppression in frequency-hopped environment. In addition, it provides the performance of a spatial smoothing technique for suppression of correlated jammers. Chapter V summarizes the thesis, states conclusions based on the simulation results, and provides recommendations for future research.

II. Literature Review

This chapter reviews the published literature on the interference rejection problems as it relates to adaptive signal processing. Adaptive filtering algorithms and adaptive beamforming for wideband interferences and for the specific case spread spectrum signals are reviewed.

2.1 Adaptive Filtering Algorithm

The first studies of minimum mean-square estimation in stochastic processes may be traced back to the late 1930s and early 1940s. Wiener formulated the continuous time linear prediction problem and derived an explicit formula for the optimum predictor. He also considered the filtering problem of estimating a process corrupted by an additive noise process. The explicit formula for the optimum estimate required the solution of an integral equation known as the *Wiener-Hoff equation* (Wiener and Hoff, 1931)

In 1947, Levinson formulated the Wiener filtering problem in discrete time. The Wiener-Hoff equation can be expressed in matrix form as follows,

$$\mathbf{R}\mathbf{w}_0 = \mathbf{p} \tag{2.1}$$

where $\mathbf{w}_0$ is the tap weight vector of the optimum Wiener filter in the form of a transversal filter, which is shown in Fig. 2.1. $\mathbf{R}$ is the correlation matrix of the tap inputs $\mathbf{u}(n)$, and $\mathbf{p}$ is the cross-correlation matrix of the tap inputs $\mathbf{u}(n)$ and the desired response $d(n)$ shown in Fig. 2.1. (Levinson, 1947).

The simple adaptive filtering *least-mean-square* (LMS) algorithm emerged as a algorithm for the operation of adaptive transversal filters in the late 1950s. The LMS algorithm was devised by Widrow and Hoff in 1959 in their study of a pattern recognition scheme known as the adaptive linear threshold logic element. The LMS algorithm is a stochastic gradient algorithm in that it iterates each tap weight in the transversal filter in the direction of the gradient of the squared

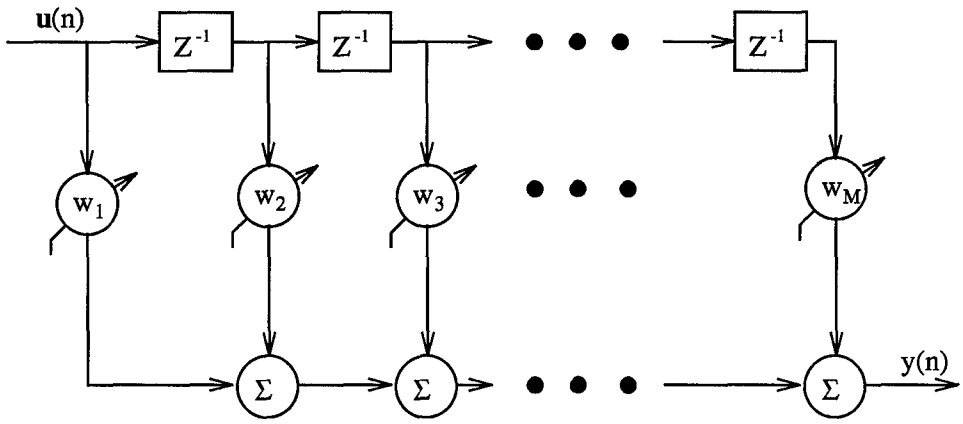

Figure 2.1 Transversal Filter

amplitude of an error signal $e(n)$ with respect to that tap weight. (Widrow, 1970). Fig. 2.2 shows a block diagram of the LMS method. The weights are adjusted or adapted in response to the data received at the transversal filter. Changing the frequency response is as simple as changing the weights. The weights in an adaptive beamformer are controlled by the LMS algorithm.

Godarn made another major contribution using Kalman filter theory to propose a new class of adaptive filtering algorithms for obtaining rapid convergence of the tap weights of a transversal filter to their optimum settings (Godard, 1974). This algorithm is referred to in the literature as the *Kalman algorithm* or *Godarn algorithm.* The Kalman algorithm is closely related to the recursive least-squares (RLS) algorithm that follows from the method of least squares (Plackett, 1950). The Kalman or RLS algorithm usually provides a much faster rate of convergence than the LMS algorithm at the expense of increased computational complexity. The desire to reduce computational complexity to a level comparable to that of the simple LMS algorithm prompted the search for a computational efficient RLS algorithm.

2.2 Adaptive Beamforming

2.2.1 General Aspect. The main object of adaptive beamforming is to put a null in the jammer direction using an adaptive filtering algorithm. The technology of adaptive beamforming

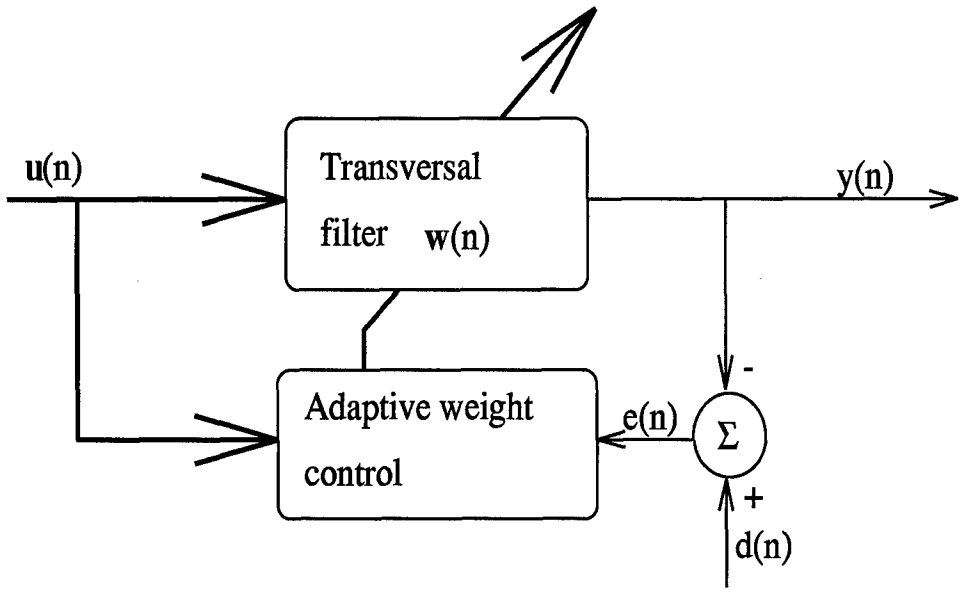

Figure 2.2 Block Diagram of LMS Algorithm

has been developed with adaptive filtering algorithms. The initial work of adaptive beamforming may be traced back to the invention of the *intermediate frequency (IF) sidelobe canceler* by Howells in the late 1950. In his historical report, Howells described a sidelobe canceler capable of automatically nulling out the effect of a jammer. The sidelobe antenna uses a *primary* (high gain) antenna and a *reference omni-directional* (low gain) antenna to form a two-element array with one degree of freedom. (Howells, 1976)

The poor performance of the delay-and-sum beamformer (the transversal filter) is due to the fact that its response along a direction of interest depends not only on the power of the incoming target but also undesirable contributions received from other sources of interference. To overcome this limitation, Capon proposed a new beamformer in which the weight vector $\mathbf{w}(n)$ is chosen to minimize the variance (i.e., average power) of the beamformer output, subject to the constraint $\mathbf{w}^H(n)\mathbf{s}(\theta) = 1$ for all n, where $\mathbf{s}(\phi)$ is a prescribed steering vector (Capon, 1969). This constrained minimization yields an adaptive beamformer with a *minimum variance distortionless response* (MVDR) which processes the desired signal from certain directions with specified gain and phases using the constraints and then minimize the output power to suppress undesired signals.

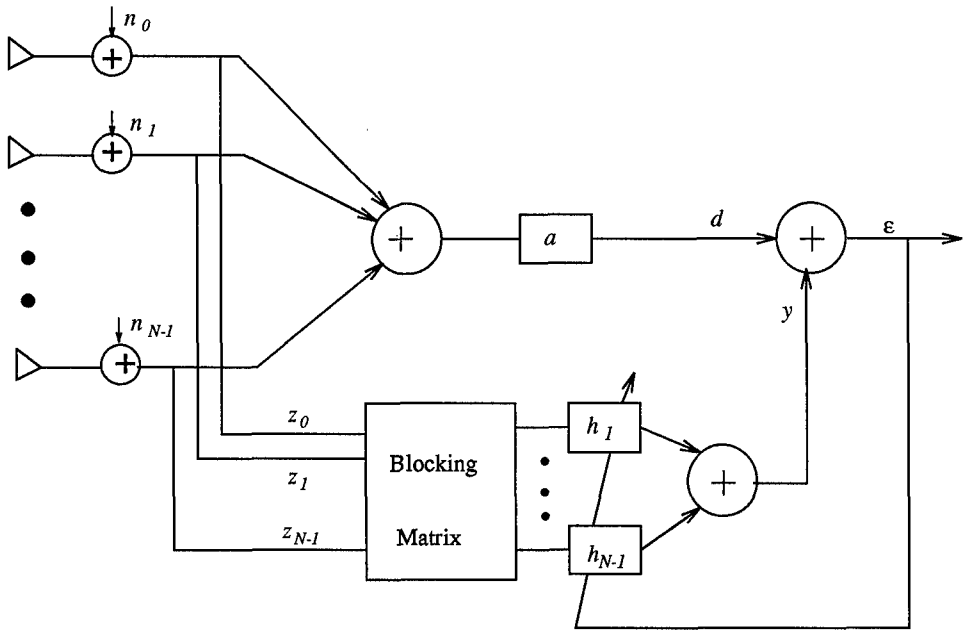

Figure 2.3 Griffiths-Jim adaptive beamformer structure

Another structure, suggested by Frost, was an adaptive algorithm designed to make the beamformer cancel everything that does not come from the desired signal direction (Frost, 1972). A linear *hard constraint* prevents cancelation from the look direction, thus avoiding the trivial zero solution. A modification of LMS algorithm to a *two-step* algorithm was used to update the coefficients. The Frost adaptive beamformer was a source of inspiration to further development.

The Widrow-McCool beamformer rearranged the Frost beamformer as a noise canceler with a slightly different constraint. The Griffiths-Jim adaptive beamformer is a modified Widrow-McCool beamformer where the constraint is included in the structure (Griffiths and Jim, 1982). In its most general form, the Griffiths-Jim structure replaces the constraints by a signal blocking matrix unit (Fig. 2.3).

2.2.2 Adaptive Beamforming for Wideband Interference Suppression. In 1967, Widrow *et al.* suggested the use of tapped delay lines in an adaptive array for wideband interference rejection (Widrow, 1967). Figure 2.4 shows the common broadband beamformer with the tapped delay lines.

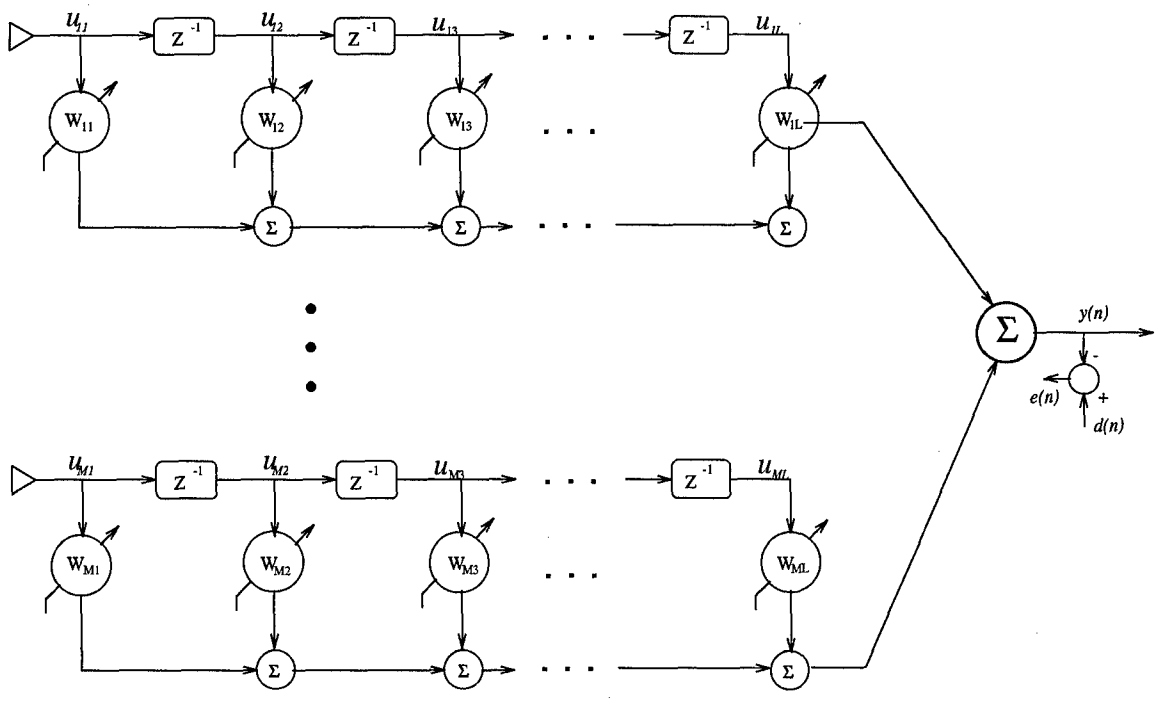

Figure 2.4 TDL Antenna Array for Wideband Jammer Suppression

This antenna is referred to TDL (Tapped Delay line) array antenna, while the antenna shown in Fig. 1.1 is referred to LMS array antenna. The study of tapped delay lines has since been done by several others. In one study, Rodgers and Compton compared the performance of a two-element array with two, three and five-tap delay lines using real weights to that of an array with a single complex weight behind each element (Rodgers, 1979). They assumed the space between taps was one quarter wavelength. In 1981, Mayhan, Simmons,, and Cummings presented a mathematical analysis of how the number of elements and the number of delay-line taps affect the interference cancelation ratio as a function of bandwidth (Mayhan, 1981). In 1983, White studied the trade-off between the number of interfering signals and the required number of auxiliary elements and delay-line taps in an Applebaum array (White, 1983). In other words, he addressed the bandwidth capability of the canceler by using tapped delay lines or simply by using more auxiliary elements.

In spite of these contributions, there was still no simple explanation in the literature for how the number of taps and the amount of delay between taps should be chosen in an adaptive

array to achieve a given bandwidth performance. In 1988, Compton addressed this question by examining a two-element adaptive array with a tapped delay-line behind each element (Compton, 1988). In the same year, he also considered the use of fast Fourier transform (FFT) processing behind the elements in adaptive arrays (Compton, 1988). However, he concluded the performance of FFT processing wasn't an improvement over tapped delay lines. He used the LMS algorithm for changing the weights in both cases.

In 1986, Buckley and Griffiths presented an adaptive broadband beamforming structure which added the Frost beamformer and TDL antenna array. This beamformer employed a gradient-based weight adjustment to minimize output variance subject to a set of J linear constraints on broadband directional derivatives in the desired look direction. Generalized sidelobe-cancelling structure was employed in which a nonadaptive beamformer operates in parallel with an adaptive beamformer (Buckley and Griffiths, 1986).

2.3 Adaptive Signal Processing in Spread Spectrum

2.3.1 Direct Sequence Spread Spectrum with Adaptive Filter. Specific implementation of an adaptive algorithm for interference suppression in Direct Sequence Spread Spectrum(DS-SS) systems has been investigated since the mid- to late-1970's. Hsu and Giordano have laid down the foundation in interference suppression in DS-SS systems (Hsu and Giordano, 1978). Their digital whitening is accomplished by using a transversal filter whose coefficients are selected by either a Wiener algorithm or a maximum entropy algorithm. Filters obtained by use of these algorithms are evaluated for various jamming and signaling conditions and are found to exhibit comparable performance over a wide range of input signal and noise ratios. The Wiener filter was implemented recursively using a least-mean-square criterion and a form of Levinson's algorithm in the actual computation.

Ketchem and Proakis further improved the results of Hsu and Giordano by combining the

interference rejection filter with its matched filter, resulting in an overall linear filter having a linear phase characteristic. They further defined the performance of the SS receiver as measured in terms of the probability of error, which was obtained by applying a Gaussian assumption on the total residual noise and interference followed by Monte Carlo simulation. Ketchum and Proakis also investigated the size of the interference suppression filter (in terms of number of taps) required to handle multiple-band interference. The frequency response improves with increasing filter order (the number of taps) in terms of providing a deeper notch at the interfering tone frequencies and less attenuation in the frequency range between notches (Ketchum and Proakis, 1932).

Saulnier has performed hardware implementations of interference suppression filters using three different transversal filter structures: charge transfer device (CTD), digital filter techniques, and surface acoustic wave (SAW) device (Saulnier et al, 1984; Saulnier et al, 1985; Saulnier, 1990). These three implementations were of the estimation-type adaptive filter. A CTD-based adaptive filter was designed using the Widrow-Hoff LMS algorithm to implement the adaptive filter architecture consisting of only two multipliers (Saulnier et al, 1984). This hardware simplification was achieved through the use of a *burst processing* technique. Saulnier, Das, and Milstein followed this work with an identical setup with a digital hardware implementation instead of the CTD (Saulnier et al, 1985). They recently performed a hardware experimentation using a SAW-based adaptive filter to perform the interference suppression (Saulnier, 1990). The primary advantage of using the SAW-based transversal filter is the availability of higher bandwidths and operating frequencies (i.e. correlation of the DS signal at RF).

The researches mentioned so far primarily performed interference suppression in the time-domain using the estimation-type predictive filter. However, throughout the 1980's, work has been accomplished in the frequency domain using transform-domain interference excisors.

In 1980, Milstein and Das provided a detailed analysis of the performance of systems in which the received signal is Fourier transformed in real time (usually with a surface acoustic wave device) and then filtered by a multiplication of the transformed signal by an appropriate transfer function

(Milstein and Das, 1980). In 1989, Gevargiz , Das and Milstein developed the transform domain processing and presented two transfer domain processing techniques. In the first technique, the narrow band interference is detected and excised in the transform domain by using an adaptive notch filter. In the second technique, the interference is suppressed using soft-limiting in the transform domain (Gevargiz et al, 1989).

Usage of a Hamming window was proposed to concentrate the energy of the narrow-band interference in a smaller fraction of the spectrum by Davidovici and Kanterakis (Davidovici and Kanterakis, 1989). The Hamming Window effectively reduced the interferences sidelobe at the expense of a wider main lobe. They presented the *overlap and save* algorithm in order to eliminate transient effects and inter-symbol interference. Due to the overlap and save method the system's filter complexity is double that of Milstein's.

Saulnier suggested the use of transform-domain adaptive filters which combined some features of the time-domain adaptive filter and the transform domain excisor (Saulnier, 1992). Weight leakage is employed to allow jammer suppression while preserving the desired DS signal, which made the desired signal power lower to indicate the high-power jammer. Bit error rate (BER) results obtained by computer simulation were presented to illustrate performance for a single-tone jammer and for a jammer consisting of a second DS signal having a lower chip rate. These results were compared to those for a transform domain excisor. Figure 2.5 show the simulation block diagram for comparison the adaptive filter with excisor in transform domain.

Another paper by Reed and Feintuch reported a comparison between implementations in the time and frequency domains (Reed and Feintuch, 1981). In addition, a thorough review paper covers many of the areas of interest within the interference rejection domain of spread spectrum communication (Milstein, 1988)

Relevant research at the Air Force Institute of Technology (AFIT) includes the following work. Shepard's 1982 master's thesis evaluated the performance of a DS (Direct Sequence) spread spectrum receiver preceded by an adaptive interference suppression (AIS) filter (Shephard, 1982).

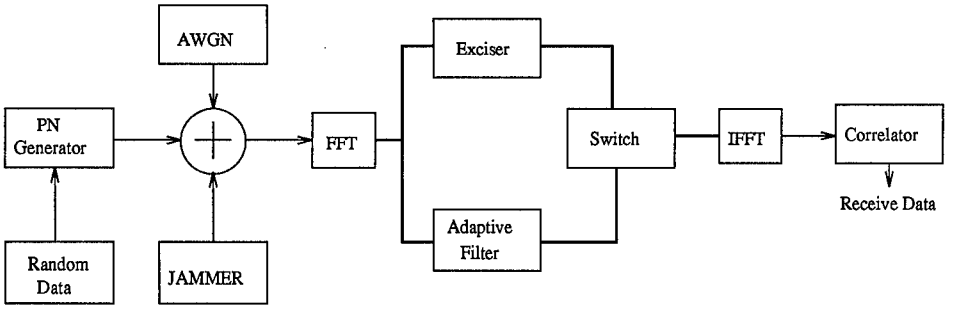

Figure 2.5 Simulation block diagram

In 1984, Way developed a simulation program to implement a 19-tap interference suppression filter for DS-SS signals. Way implemented a different adaptive algorithm: a *soft-constraint* version of the least-mean-square (LMS) algorithm. He examined the filter's effectiveness versus single-tone jammers and frequency hopping tone jammers. He likewise evaluated the performance of the filter via SNR improvement (Way, 1984). In 1990, Mikulanicz provided a performance evaluation of a 128-tap PTF (Programmed Transversal Filter). He demonstrated the effectiveness in creating assorted FIR bandpass filter responses using the rectangular, Hamming , and Hanning window distribution (Mikulanicz, 1990).

2.3.2 Frequency Hopping Spread Spectrum with Adaptive Beamforming. Adaptive beamforming and frequency hopping (FH) over a wide band are two of the most powerful methods for interference rejection. The application of FH modulation in an antenna array will improve substantially the SINR (Signal to Interference plus Noise Ratio) as a consequence of the increase of the resolution and the interference rejection.

Compton studied the adverse effects of FH modulation in an adaptive array based on the LMS algorithm (Compton, 1985). Bakhru proposed a specific method for adaptive arrays using FH signals, so called maximum algorithm. It is an adaptive algorithm that suppresses interference before it enters the receivers of a frequency hopping communication system. Thus, the algorithm provides a processing gain that supplements the inherent processing gain of the frequency hopping

system. The algorithm discriminates between the desired signal and the interference on the basis of the distinct spectral characteristics of frequency hopping signals. The maximum algorithm is so named because the desired signal is enhanced and the interference is suppressed simultaneously by parallel sub-processors. The algorithm is blind in the sense that neither the direction of the desired signal nor its waveform needs to be known (Bakhru and Torrieri, 1984). Nonetheless any adaptive algorithm presents some discontinuities when used with FH modulated signals. The reason is that the changes in the signal frequency due to FH are seen by the algorithm as changes in the direction of arrival.

Torrieri suggested three different techniques of frequency compensation for the maximum algorithm to solve this problem (Torrieri and Bakhru, 1987). The parameter dependent processing uses an adaptive filter behind each antenna element. Each adaptive filter has enough adjustable parameters to allow the formation of nulls in the directions of the sources of interference for all frequencies. This processing is the most complicated to implement but presents faster convergence. Spectral processing is based upon dividing that total hopping band into a number of spectral regions called bins and adapting the weight vector independently each time the carrier frequency of the frequency hopping signal is in one of the bins. This processing is the simplest to implement but the achieved improvement is not significant. An anticipative adaptive system begins adaptation toward the optimal weights for a carrier frequency before that frequency is transmitted. A time advanced frequency hopping replica hops approximately one hop duration ahead of the replica hops for dehopping the received signal. While the main adaptive filter produces the output, the auxiliary filter adapts its weights to suppress the next carrier frequency. After each hop, the weight values associated with the new carrier frequency are transferred from the auxiliary filter to the main filter. Anticipate processing provides the fastest convergence to the steady state, but exhibits the largest variation in the steady state SINR.

Najar and Lagunas further developed the anticipative processing by adding a generalized sidelobe canceller (GSC). His approach to the optimum solution consists two different stages. The

first stage, named the anticipative stage, is devoted to cancel interference at fixed frequencies that are already present or active at the frequency of interest at the hop time. The second state, named GSC stage, is used for combating interferences that are not present at the frequency of interest at the time of the frequency hop (Najar and Lagunas, 1995). They showed the grating lobe is reduced significantly in the mean array factor when the FH signals is used with antenna array.

2.4 Conclusion

This chapter presented a brief historical review of developments in three areas that are closely related in so far as the subject matter of this research. Those areas are adaptive filtering algorithm, adaptive beamforming for wideband interference suppression. Many researchers have investigated the adaptive filters for narrowband interference suppression and adaptive beamforming for wideband interference suppression. Special attention was devoted to adaptive filters in the DS-SS system. In the FH-SS signal environments, the researches relating adaptive antenna array and FH modulation for interference suppression have been developed because the antenna array and FH modulation is closely related with each other. In the next chapter, we derive the theories of adaptive filter and beamforming.

III. Adaptive Signal Processing

3.1 Background

3.1.1 Overview. This chapter discusses the similarity of temporal and spatial filters. Then, the time domain adaptive filters are considered using LMS adaptive algorithm and the spatial filter (i.e., adaptive beamforming) is discussed using the linear constrained minimum variance (LCMV) algorithm with generalized sidelobe canceller (GSC). An optimum value and LMS estimate of weights are also computed. Finally, the adaptive beamformer in the presence of correlated signals is considered.

3.1.2 Notation. Since vectors and matrices are used throughout this research, it is important to establish the notation that will be used. Vectors are always represented with lowercase boldface symbols, for example, $\mathbf{w}$, and are assumed to be column vector. Matrices are denoted by boldface upper case symbols, for example $\mathbf{C}$. Superscripts $*$, T, H, and -1 represent complex conjugate, transpose, complex conjugate transpose, and matrix inverse, respectively.

3.1.3 Definition, Signals may be classified as either narrowband or wideband. Narrowband is defined in terms of the fractional bandwidth of the signal. The fractional bandwidth is the signal bandwidth as a percentage of the carrier frequency. Signals whose fractional bandwidths are much less than 2 percent will be characterized as narrowband, while those with fractional bandwidths much greater than 2 percent will be called wideband (Haykin and Steinhardt, 1992).

3.1.4 Temporal Filter versus Spatial Filter. Although the temporal filter problem in additive receiver noise and the spatial filter problem corrupted by additive sensor noise arise in different application areas, their mathematical formulations and procedures for their solution are indeed similar.

For the temporal filtering of data, we propose using a transversal filter of length M as indicated

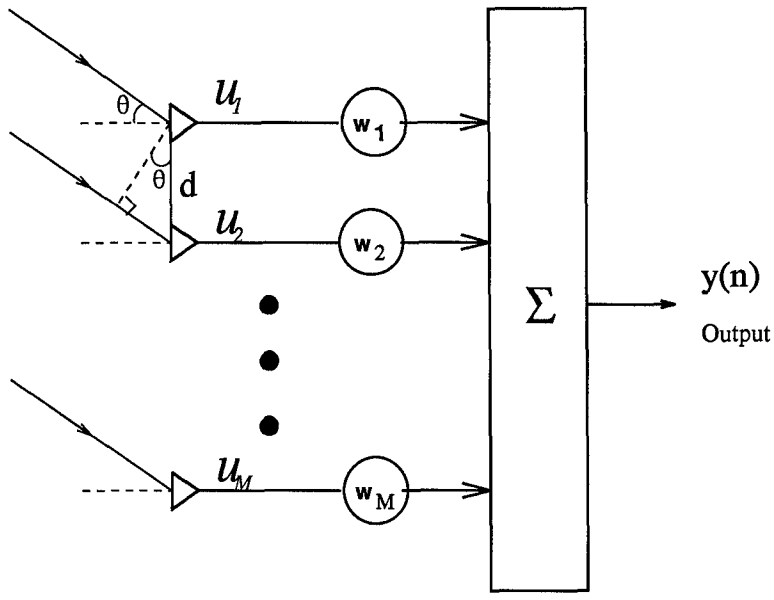

Figure 3.1 Linear Array of Sensors for Spatial Processing

in Fig. 2.1. The filter output, in response to the tap inputs, is given by

$$y(n) = \sum_{k=0}^{M-1} w_k^* u(n-k), \tag{3.1}$$

where w_k is kth tap weight and $u(n)$ is tap input in time n. For the special case of a *sinusoidal excitation*

$$u(n) = e^{j\omega n}, \tag{3.2}$$

we may rewrite Eq. 3.1 as

$$y(n) = e^{j\omega n} \sum_{k=0}^{M-1} w_k^* e^{-j\omega k}, \tag{3.3}$$

where ω is the angular frequency of the excitation, which is normalized with respect to the sampling rate.

Consider next the spatial analog of this temporal problem. Fig. 3.1 depicts a receiving *linear array* of uniformly spaced sensors labeled 1,$\cdots$, M. Let d denote the separation between adjacent elements of the array. In Fig. 3.1 a single plane wave was impinging on the array at angle of

incidence θ, measured with respect to the boresight. It is assumed that the inter-element distance is a half wavelength so as to avoid the appearance of grating lobes (Skolnik, 1980). The resulting beamforming output is given by

$$y(n) = u(n) \sum_{k=0}^{M-1} w_k^* e^{-jk\phi}, \tag{3.4}$$

where the direction of arrival is defined by the electrical angle $\phi = \frac{2\pi d}{c} \sin\theta$ that is related to the angle of incidence θ and the antenna interelements distance d, $u(n)$ is the electrical signal picked up by the antenna element labeled u_1 in Fig. 3.1 that is treated as the point of reference, and the w_k denote the element weights of the beamformer. The important point to note is the mathematical similarity between the temporal model of Eq. 3.3 and the spatial model of Eq. 3.4.

3.2 Adaptive Filter : Temporal Filter

An adaptive filter converges to the optimum Wiener solution in a stationary environment. The LMS algorithm starts from some predetermined set of initial conditions and is self-designing. It relies for its operation on a recursive algorithm, which makes it possible for the filter to perform satisfactorily in an environment where complete knowledge of the relevant signal characteristics is not available. On the other hand, the design of a Wiener filter requires prior information about the statistics of the data to be processed (Widrow, 1985). For real-time operation, this procedure has the disadvantage of requiring excessively elaborate and costly hardware.

3.2.1 Input Signal and Weight Vector. The operation of a linear adaptive filtering algorithm involves two basic processes: (1) a *filtering* process designed to produce an output in response to sequence of input data, and (2) an *adaptive* process. The transversal filter type is used, which referred to as a tapped-delay line filter, as depicted in Fig. 2.1. For the transversal filter, we obtain

the input-output relationships as follows:

$$y(n) = \sum_{k=0}^{M-1} w_k^* u(n-k). \tag{3.5}$$

In vector notation, this can be written as

$$y(n) = \mathbf{w}^H \mathbf{u}(n), \tag{3.6}$$

where the input and weight vector are expressed by vector notation as,

$$\begin{aligned} \mathbf{u}(n) &= [u(n), u(n-1), \cdots, u(n-M+1)]^T \\ \mathbf{w} &= [w_1, w_2, \cdots, w_M]^T. \end{aligned}$$

3.2.2 Minimum Mean Squared Error. For the case of stationary inputs, the *performance function* is defined as the *mean square error* which is the mean squared value of the difference between the desired response and the transversal filter output. As in Fig. 2.2 the error signal is

$$\begin{aligned} e(n) &= d(n) - y(n) \\ &= d(n) - \mathbf{w}^H \mathbf{u}. \end{aligned}$$

Squaring the error signal to obtain the squared error, one obtains

$$e(n)^2 = d(n)^2 + \mathbf{w}^H \mathbf{u}\mathbf{u}^H \mathbf{w} - 2d(n)\mathbf{u}^H \mathbf{w}. \tag{3.7}$$

Then taking the expected value, the MSE (Mean Squared Error) becomes

$$MSE = E\{d(n)^2\} + \mathbf{w}^H E\{\mathbf{u}\mathbf{u}^H\}\mathbf{w} - 2E\{d(n)\mathbf{u}^H\}\mathbf{w}$$

$$= E\{\mathbf{d}^2\} + \mathbf{w}^H\mathbf{R}\mathbf{w} - 2\mathbf{p}\mathbf{w}, \tag{3.8}$$

where $\mathbf{R}$ is defined as the square matrix :

$$\mathbf{R} = E\{\mathbf{u}\mathbf{u}^H\}. \tag{3.9}$$

Correspondingly, $\mathbf{p}$ is denoted by the M-by-1 cross correlation vector between the tap inputs of the filter and the desired response $d(n)$:

$$\mathbf{p} = E\{\mathbf{u}d(n)^*\}. \tag{3.10}$$

Many useful adaptive processes work by seeking the weight vector which minimizes the performance function using gradient search methods. The gradient of the mean squared error performance surface, designated ∇, can be obtained by differentiating Eq. 3.8 to obtain the column vector :

$$\nabla = \frac{\partial MSE}{\partial \mathbf{w}} = 2\mathbf{R}\mathbf{w} - 2\mathbf{p}.$$

3.2.3 LMS Adaptation Algorithm. Since the gradient vector must be estimated from the available data, the simplest estimate of gradient vector is the instantaneous estimates based on sample values of the tap-input vector and desired response :

$$\hat{\nabla} = 2\hat{\mathbf{R}}\hat{\mathbf{w}} - 2\hat{\mathbf{p}} = 2\mathbf{u}(n)\mathbf{u}^H(n)\hat{\mathbf{w}} - 2\mathbf{u}(n)d^*(n)$$

Let $\hat{\mathbf{w}}(n)$ denote the value of the tap weight vector at time n. The updated value of the tap-weight vector at time $n+1$ is computed by using the simple recursive relation

$$\hat{\mathbf{w}}(n+1) = \hat{\mathbf{w}}(n) + \mu\mathbf{u}(n)[d^*(n) - \mathbf{u}^H(n)\hat{\mathbf{w}}] \tag{3.11}$$

3.2.4 Summary. Adaptive temporal filter have a built in mechanism for the automatic adjustment of its weight in response to statistical variations of the environment in which the filter operates. The weight adjustments are made iteratively by using standard adaptive algorithms that seeks an optimum value. The filter input consisting of a vector of uniformly spaced samples taken from a long data stream is used to determine weights that minimize the performance function calculated by gradient methods. The updated weight vector is computed by using the simple recursive relation as depicted in Eq. 3.11.

3.3 Adaptive Beamforming

3.3.1 Introduction. A *beamformer* is a signal processor used in conjunction with a set of antennas that are spatially separated. The beamformer output is simply a weighted combination of the outputs of the set of antennas. Usually the goal of beamforming is spatial filtering, that is, separation of signals which have similar temporal frequency content but originate from different spatial locations. Here, we use digital beamforming that detects and digitizes the received signal at the element level via discrete processing techniques.

In an *adaptive beamformer* the weights are adjusted or adapted in response to the data received at the antennas to optimize the beamformer's spatial response. Changing the beamformer's spatial response is as simple as changing the weights. The weights in an adaptive beamformer are controlled by an *adaptive algorithm.* All adaptive antennas to date have been *arrays*, because the pattern of an array is easily controlled by adjusting the amplitude and phase of the signal from each element before combining the signals. Adaptive antennas are useful in radar and communication systems that are subject to interference and jamming. They change their patterns in a way that optimizes the signal-to-interference-plus-noise ratio at the array output.

3.3.2 Input Signal and Weight Vector . Fig. 1.1 illustrated a beamformer typically used for processing narrowband signals. The antenna outputs are sampled and are represented in discrete time for notational convenience and consistency. The M antenna sensor outputs are weighted and then summed to compute the beamformer output. This method is called as delay-and-sum beamformer. Each sensor is assumed to have any necessary receiver electronics and an A/D converter. The discrete time delay and sum beamformer $y(n)$ is given by

$$y(n) = \sum_{m=1}^{M} w_m^* u_m(n), \tag{3.12}$$

where w_m and $u_m(n)$ are the weight and input data, respectively, in the mth antenna channel.

A beamforming structure commonly utilized to process wideband signals is depicted in Fig. 2.4. In this case there are tap delay lines in each channel. The output, $y(n)$ is expressed as

$$y(n) = \sum_{m=1}^{M-1} \sum_{l=0}^{L-1} w_{m,l}^* u_{m,l}(n), \tag{3.13}$$

where L is the number of taps in each of the M channels and $w_{m,l}$ is the weight applied to the lth tap of the mth channel. This means that the output of each sensor is then passed through a FIR filter having L weights. The time domain filtering is intended to provide some rejection of interference not lying in the proper temporal frequency region. The resulting FIR filter describing the relation between array input and output has tap values equal to the sum of component-filter tap values occurring at the temporal delay. Once each antenna sensor's output delayed by an amount appropriate for the propagation direction is passed through a FIR filter whose weights are selected individually.

Both Eq. 3.12 and Eq. 3.13 are compactly written as the inner product

$$y(n) = \mathbf{w}^H \mathbf{u}(n), \tag{3.14}$$

where $\mathbf{w}$ is the vector of beamformer weights and $\mathbf{u}(n)$ is vector of data.

In vector notation, the complex conjugate transpose of the N-dimensional vector of signals contained in the beamformer at the nth time sample is given by

$$\mathbf{u}^H(n) = [\mathbf{u}_0^H(n), \quad \mathbf{u}_1^H(n), \quad \cdots, \quad \mathbf{u}_{L-1}^H(n)]. \tag{3.15}$$

Let the dimension of $\mathbf{w}$ and $\mathbf{u}(n)$ be N where $N = M$ in the narrowband case (Eq. 3.12) and $N = ML$ in the wideband case (Eq. 3.13). Note that the form of both equation implies that the complex conjugate of the weights are actually applied to the data samples within the beamformer.

3.3.3 Antenna Array Response Vector. In the narrowband case, the frequency response of an antenna array with antenna element weights w_m and a propagation delay T_p seconds is given by,

$$r(\omega_c, \theta_p) = \mathbf{w}^H \mathbf{d}(\omega_c, \theta_p), \tag{3.16}$$

where

$$\begin{aligned} \mathbf{w} &= [w_1, \quad w_2, \quad \cdots, \quad w_M]^H. \\ \mathbf{d}(\omega_c, \theta_p) &= [1 \quad e^{j\omega_c T_p} \quad e^{j2\omega_c T_p} \quad \cdots \quad e^{j(M-1)\omega_c T_p}]^H. \end{aligned}$$

$r(\omega_c, \theta_p)$ represents the response of the antenna to frequency ω_c and $\mathbf{d}(\omega_c, \theta_p)$ is a vector describing the phase at each element in the antenna array relative to the element associated with w_1. T_p is $\frac{d}{c}\sin(\theta_p)$, where c is propagation velocity and d is antenna interelement space and θ_p is incidental direction for signals.

Assume that the array spatially samples a propagating wave of frequency ω_c in the direction θ_p. For convenience let the phase due to propagation be referenced to zero at the first sensor and

let $a_1(\theta_p, \omega_c)$ be the response of the first antenna element as a function of direction and frequency. Assuming identical antennas,

$$\begin{aligned} y(n) &= u(n) \sum_{m=0}^{M-1} w_m a_1(\theta_p, \omega_c) e^{-j\omega_c m T_p} \\ &= u(n) r(\theta_p, \omega_c). \end{aligned}$$

The term $r(\theta_p, \omega_c)$ is the beamformer response and the elements of $\mathbf{d}(\theta_p, \omega_c)$ correspond to the complex exponentials $a_1(\theta_p, \omega_c) e^{-j\omega_c(m-1)T_p}$ $1 \leq m \leq M$. The vector $\mathbf{d}(\theta_p, \omega_c)$ is termed the *array response vector.* Assuming $a_1(\theta_p, \omega_c)$=1, $\mathbf{d}(\theta_p, \omega_c)$ is written as

$$\mathbf{d}(\theta_p, \omega_c) = [1 \quad e^{j\omega_c T_p} \quad e^{j2\omega_c T_p} \quad \cdots \quad e^{j(M-1)\omega_c T_p}]^H. \tag{3.17}$$

In this case we identify the relationship between temporal frequency ω in $\mathbf{d}(\omega)$ (FIR filter) and direction θ_p (beamformer) as $w = w_c \frac{d}{c} \sin(\theta_p)$.

3.3.4 Basic Concept of LCMV Beamforming .

3.3.4.1 Linear Constraints. We will use the constraint, in which the beamformer response at a specified frequency and direction of desired signal must meet some gain and phase requirements. The response is constrained at radian frequency ω_c and angle θ_p as

$$\mathbf{w}^H \mathbf{d}(\theta_p, \omega_c) = f_1, \tag{3.18}$$

where f_1 is the desired complex response. Several linear constraints can be expressed as,

$$\mathbf{C}^H \mathbf{w} = \mathbf{f}, \tag{3.19}$$

where $\mathbf{C}$ is the constraint matrix and $\mathbf{f}$ is the response vector.

In the narrowband case, the matrix $\mathbf{C}$ is chosen to contain r linear constraints so the above equation represents r linearly independent columns in M unknowns. The weight vector $\mathbf{w}$ has length M, while $\mathbf{C}$ is an M $\times r$ matrix. If $M = r$, then $\mathbf{w}$ is uniquely determined by the constraints. To ensure there is a $\mathbf{w}$ which satisfies the constraints, r is chosen to be less than M. Here we consider the desired signal gain-only constraint,

$$\mathbf{C} = \mathbf{d}(\theta_p, \omega_c) \tag{3.20}$$

where

$$\mathbf{d}(\theta_p, \omega_c) = [1 e^{j\omega_c T_p} \quad e^{j2\omega_c T_p} \quad \dots \quad e^{j(M-1)\omega_c T_p}]^H, \tag{3.21}$$

$\mathbf{d}(\theta_p, \omega_c)$ is $M \times 1$ and T_p is $\frac{c}{d} \sin\theta_p$, c is propagation velocity and d is antenna interelement space and θ_p is incidental direction for signals.

In the wideband case, for steer-direction gain-only constraints,

$$\mathbf{f} = [1, 0 \dots, 0]^T \tag{3.22}$$

$$\mathbf{C} = \begin{pmatrix} \mathbf{d}(\theta_p, \omega_c) & \mathbf{0}_M & \dots & \mathbf{0}_M \\ \mathbf{0}_M & \mathbf{d}(\theta_p, \omega_c) & \dots & \mathbf{0}_M \\ \vdots & \vdots & \ddots & \vdots \\ \mathbf{0}_M & \mathbf{0}_M & \dots & \mathbf{d}(\theta_p, \omega_c) \end{pmatrix} \tag{3.23}$$

The $\mathbf{d}(\theta_p, \omega_c)$ is $M \times 1$, and the column vector $\mathbf{0}_M$ contains M zeros. The L-dimensional gain vector $\mathbf{f}$ describes the frequency response of the beamformer to a signal impinging on the array from the desired look direction (Frost, 1972). The constraint matrix C is $ML \times L$ dimensional. If $\mathbf{f}$ is a vector which contains a single one and $L - 1$ zeros, then the temporal response will be flat and the system will not distort any signal incident on the array from the look direction, θ_p.

3.3.4.2 LCMV Approach. Variance minimization effectively minimizes the interference and noise power at the beamformer output while the constraints preserve the signal of interest. Formally stated, we derive

$$\min_{\mathbf{w}}(P_o) = \min_{\mathbf{w}}(\mathbf{w}^H \mathbf{R}_u \mathbf{w}), \quad \textit{subject to} \quad \mathbf{C}^H \mathbf{w} = \mathbf{f}, \tag{3.24}$$

where P_o represents the output power. $\mathbf{R}_u = E\{\mathbf{u}\mathbf{u}^H\}$ represents the exact covariance matrix of the received signal $\mathbf{u}$. The Eq. 3.24 is to find out the weight vector for minimum output P_o. The solution is derived in Appendix A using *Lagrange multipliers*, given by,

$$\mathbf{w}_{opt} = \mathbf{R}_u^{-1}\mathbf{C}[\mathbf{C}^H \mathbf{R}_u^{-1}\mathbf{C}]^{-1}\mathbf{f}. \tag{3.25}$$

The inverse exists because $\mathbf{C}$ is full rank and $\mathbf{R}_u$ is positive definite because the data always contains an uncorrelated noise component.

3.3.5 LCMV-GSC Beamformer .

3.3.5.1 Basic Concept of GSC. Fig. 3.2 shows the generalized sidelobe canceler (GSC) block diagram. Note that the input vector is the M-dimensional stacked data vector $\mathbf{u}(n)$ for the narrowband signal. For steer direction gain only constraints ($r = 1$), the linear constraint is defined in Eq. 3.20. Let the columns of an $M \times (M - r)$ matrix $\mathbf{C}_a$ be defined as a basis for the orthogonal complement of the space spanned by the columns of matrix $\mathbf{C}$ which is composed of orthonormal columns. Using the definition of an orthogonal complement, we may thus write

$$\mathbf{C}^H \mathbf{C}_a = \mathbf{0}. \tag{3.26}$$

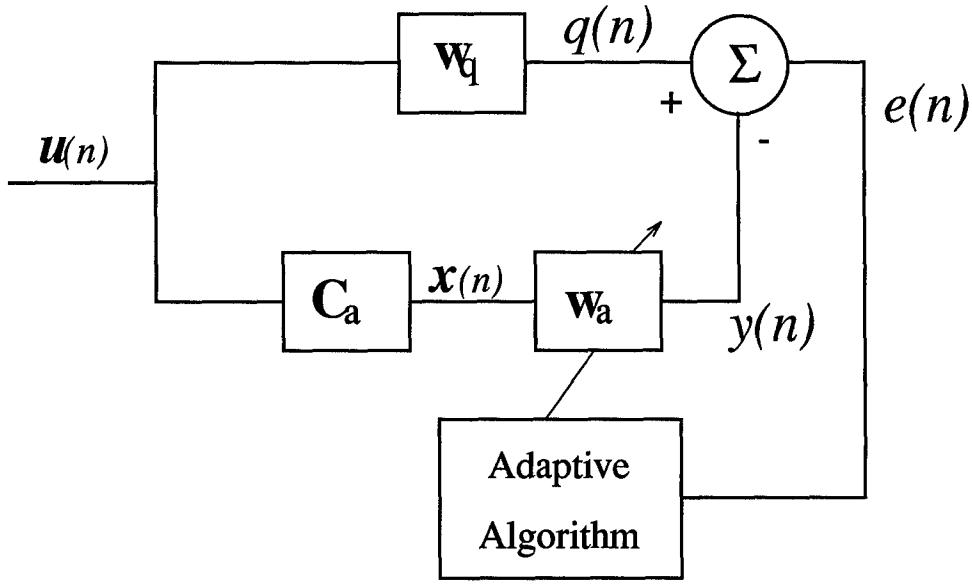

Figure 3.2 Block Diagram for a Generalized Side-Lobe Canceler (GSC)

Define the M-by-M partitioned matrix

$$\mathbf{U} = [\mathbf{C} : \mathbf{C}_a], \tag{3.27}$$

whose columns span the entire M-dimensional signal space.

Let the $\mathbf{v}$ be partitioned in compatible to Eq. 3.27,

$$\mathbf{v} = \begin{bmatrix} \mathbf{q} \\ \cdots \\ -\mathbf{w}_a \end{bmatrix}. \tag{3.28}$$

where $\mathbf{q}$ is r-by-1 vector, and the $(M-r)$-by-1 vector $\mathbf{w}_a$ is the portion of the weight vector $\mathbf{w}$ that is not affected by the constraints.

So that the M-by-1 weight vector is represented by $\mathbf{U}$ and $\mathbf{v}$ where

$$\mathbf{w} = \mathbf{U}\mathbf{v}, \tag{3.29}$$

and $\mathbf{U}^{-1}$ exists because the determinant $\mathbf{U}$ is not zero,

$$\mathbf{v} = \mathbf{U}^{-1}\mathbf{w}. \tag{3.30}$$

We may use Eq. 3.27 and Eq. 3.28 in Eq. 3.29 to obtain

$$\begin{aligned} \mathbf{w} &= [\mathbf{C} : \mathbf{C}_a] \begin{bmatrix} \mathbf{q} \\ \dots \\ -\mathbf{w}_a \end{bmatrix} && (3.31) \\ &= \mathbf{C}\mathbf{q} - \mathbf{C}_a\mathbf{w}_a. && (3.32) \end{aligned}$$

Now, inserting Eq. 3.32 into Eq. 3.19, we obtain

$$\mathbf{C}^H\mathbf{C}\mathbf{q} - \mathbf{C}^H\mathbf{C}_a\mathbf{w}_a = \mathbf{f}. \tag{3.33}$$

Through Eq. 3.26, the Eq. 3.33 will be,

$$\mathbf{C}^H\mathbf{C}\mathbf{q} = \mathbf{f}. \tag{3.34}$$

Therefore, solving for the vector $\mathbf{q}$,

$$\mathbf{q} = (\mathbf{C}^H\mathbf{C})^{-1}\mathbf{f}, \tag{3.35}$$

which shows the linear constraint doesn't affect $\mathbf{w}_a$.

Define the non-adaptive beamformer component represented by, which is the first part of Eq. 3.32,

$$\mathbf{w}_q = \mathbf{C}\mathbf{q} = \mathbf{C}(\mathbf{C}^H\mathbf{C})^{-1}\mathbf{f}. \tag{3.36}$$

Substituting Eq. 3.36 into Eq. 3.32 yields the follow equation relating,

$$\mathbf{w} = \mathbf{w}_q - \mathbf{C}_a\mathbf{w}_a. \tag{3.37}$$

Substituting Eq. 3.37 into Eq. 3.19,

$$\mathbf{C}^H\mathbf{w}_q - \mathbf{C}^H\mathbf{C}_a\mathbf{w}_a = \mathbf{f}. \tag{3.38}$$

By virtue of Eq. 3.26,

$$\mathbf{C}^H\mathbf{w}_q = \mathbf{f}, \tag{3.39}$$

which shows the non-adaptive component $\mathbf{w}_q$ of the weights $\mathbf{w}$ satisfies the linear constraints. The weight vector $\mathbf{w}_q$ is termed the quiescent weight vector because it is optimum LCMV weight vector when the environment is quiet. As the results, the GSC has only one data dependent element $\mathbf{w}_a$ due to the fact that both the quiescent beamformer $\mathbf{w}_q$ in the upper path and the blocking matrix $\mathbf{C}_a$ in the lower path depend only on the constraint equations.

Note that the constraint does not affect $\mathbf{w}_a$ because $\mathbf{w}_a$ embodies the available degrees of freedom in $\mathbf{w}$. The second term on the right side of Eq. 3.37 is incorporated in the lower branch of the GSC and is essentially an unconstrained adaptive beamforming , which have the $M - r$ the number of adaptive weights. The constraint matrix $\mathbf{C}$ preserves the desired signal. But the matrix $\mathbf{C}_a$ blocks any portion of the data that is constrained in the space spanned by the columns of $\mathbf{C}$. Consequently, no part of the received signal subspace is allowed to pass through the lower branch of the GSC. The matrix $\mathbf{C}_a$ is for this reason called the *blocking matrix.*

3.3.5.2 LMS Estimate of Weights for LCMV-GSC Beamforming. We perform the unconstrained minimization of the mean-squared value to minimize the effect of the jammer by adjusting the weight vector $\mathbf{w}_a$ using LMS algorithm. According to Eq. 3.14, the beamformer

output $y(n)$ is expressed by the inner product,

$$y(n) = \mathbf{w}^H \mathbf{u}(n), \tag{3.40}$$

where $u(n)$ is the electrical signal picked up by first antenna element of the linear array in Fig. 1.1 and Fig. 2.4 at time n. By substituting Eq. 3.37 in Eq. 3.40, the beamformer output in Fig. 3.2 is,

$$y(n) = \mathbf{w}_q^H \mathbf{u}(n) - \mathbf{w}_a^H \mathbf{C}_a^H \mathbf{u}(n). \tag{3.41}$$

In Eq. 3.41, the inner product $\mathbf{w}_q^H \mathbf{u}(n)$ plays the role of quiescent response:

$$q(n) = \mathbf{w}_q^H \mathbf{u}(n). \tag{3.42}$$

Similary, the matrix product $\mathbf{C}_a^H \mathbf{u}(n)$ plays the role of input vector for the adjustable weight vector $\mathbf{w}_a$. To emphasize this point, we let

$$\mathbf{x}(n) = \mathbf{C}_a^H \mathbf{u}(n). \tag{3.43}$$

We are now ready to formulate the LMS algorithm for the adaption of weight vector $\mathbf{w}_a(n)$ in the GSC. The derivation is based on Section 3.2, especially Eq. 3.11. We may write

$$\begin{aligned} \mathbf{w}_a(n+1) &= \mathbf{w}_a(n) + \mu \mathbf{C}_a^H \mathbf{u}(n) e^*(n) \\ &= \mathbf{w}_a(n) + \mu \mathbf{C}_a^H \mathbf{u}(n) (\mathbf{w}_q^H \mathbf{u}(n) - \mathbf{w}_a^H \mathbf{C}_a^H \mathbf{u}(n))^* \\ &= \mathbf{w}_a(n) + \mu \mathbf{C}_a^H \mathbf{u}(n) \mathbf{u}(n)^H (\mathbf{w}_q - \mathbf{C}_a \mathbf{w}_a(n)). \end{aligned} \tag{3.44}$$

3.3.5.3 Optimum Value of Weights for LCMV-GSC Beamforming. Based upon this explanation of the GSC, we can now express the LCMV beamformer with the following

unconstrained minimization equation (Haykin and Steinhardt, 1992),

$$P_o = \min_{\mathbf{w}_a}(\mathbf{w}_q - \mathbf{C}_a\mathbf{w}_a)^H\mathbf{R}_u(\mathbf{w}_q - \mathbf{C}_a\mathbf{w}_a), \tag{3.45}$$

or

$$P_o = \min_{\mathbf{w}_a}(\mathbf{w}_q^H\mathbf{R}_u\mathbf{w}_q - \mathbf{w}_q^H\mathbf{R}_u\mathbf{C}_a\mathbf{w}_a - \mathbf{w}_a^H\mathbf{C}_a^H\mathbf{R}_u\mathbf{w}_q + \mathbf{w}_a^H\mathbf{C}_a^H\mathbf{R}_u\mathbf{C}_a\mathbf{w}_a). \tag{3.46}$$

Completing the square we have

$$\begin{aligned} P_o = \min_{\mathbf{w}_a} \quad & [\mathbf{w}_a - (\mathbf{C}_a^H\mathbf{R}_u\mathbf{C}_a)^{-1}\mathbf{C}_a^H\mathbf{R}_u\mathbf{w}_q]\mathbf{C}_a^H\mathbf{R}_u\mathbf{C}_a[\mathbf{w}_a - (\mathbf{C}_a^H\mathbf{R}_u\mathbf{C}_a)^{-1}\mathbf{C}_a^H\mathbf{R}_u\mathbf{w}_q] \\ & + \mathbf{w}_q^H\mathbf{R}_u\mathbf{w}_q - \mathbf{w}_q^H\mathbf{R}_u\mathbf{C}_a(\mathbf{C}_a^H\mathbf{R}_u\mathbf{C}_a)^{-1}\mathbf{C}_a^H\mathbf{R}_u\mathbf{w}_q. \end{aligned} \tag{3.47}$$

The matrix $\mathbf{C}_n$ is full rank and $\mathbf{R}_u$ is positive definite so $\mathbf{C}_n^H\mathbf{R}_u\mathbf{C}_n$ is positive definite and the inverse exists. Eq. 3.47 is minimized when

$$\mathbf{w}_a = (\mathbf{C}_a^H\mathbf{R}_u\mathbf{C}_a)^{-1}\mathbf{C}_a^H\mathbf{R}_u\mathbf{w}_q. \tag{3.48}$$

The minimum output power is obtained using this set of weights and is given by

$$P_0 = \mathbf{w}_q^H\mathbf{R}_u\mathbf{w}_q - \mathbf{w}_q^H\mathbf{R}_u\mathbf{C}_a(\mathbf{C}_a^H\mathbf{R}_u\mathbf{C}_a)^{-1}\mathbf{C}_a^H\mathbf{R}_u\mathbf{w}_q. \tag{3.49}$$

Suppose $\mathbf{u} = \mathbf{s} + \mathbf{j}$ where $\mathbf{s}$ is the component of the data due to the desired signal and $\mathbf{j}$ is the component due to jammer signal. Assume that the constraints are chosen to preserve the desired signal, that is, $\mathbf{s}$ lies in the space spanned by the columns of $\mathbf{C}$ so $\mathbf{C}_a^H\mathbf{R}_s = 0$. This implies that the beamformer output is

$$y = \mathbf{w}_q^H\mathbf{s} + (\mathbf{w}_q - \mathbf{C}_a\mathbf{w}_a)^H\mathbf{j}. \tag{3.50}$$

If we further assume that the signal and interference are uncorrelated, then the output power or variance is expressed as

$$E\{|y|^2\} = \mathbf{w}_q^H \mathbf{R}_s \mathbf{w}_q + \mathbf{w}^H \mathbf{R}_j \mathbf{w}, \tag{3.51}$$

where $\mathbf{w}^H \mathbf{R}_j \mathbf{w}$ is the jamming signal component of the output power. Therefore, minimizing the total output power subject to $\mathbf{C}^H \mathbf{w} = \mathbf{f}$ is equivalent to minimizing the jammer output power subject to the same constraints. Substitute the GSC representation for $\mathbf{w}$ into Eq. 3.51 with $\mathbf{w}_a$ given by Eq. 3.48 and utilize the identity $\mathbf{C}_a^H \mathbf{R}_s = \mathbf{0}$ to express the minimum output power P_o as a sum of signal output power, P_s, and jammer output power, P_j where

$$\begin{aligned} P_s &= \mathbf{w}_q^H \mathbf{R}_s \mathbf{w}_q \\ P_n &= \mathbf{w}^H \mathbf{R}_j \mathbf{w}. \end{aligned} \tag{3.52}$$

The mean squared error (MSE) between the desired signal and the beamformer output is easily derived using the GSC representation. We assume the constraints are chosen so that the beamformer output in the absence of interference and noise is equal to the desired signal, y_d. that is, $y_d = \mathbf{w}_q^H \mathbf{s}$. Defining the MSE as

$$MSE = E\{|y_d - y|^2\}, \tag{3.53}$$

and substituting Eq. 3.50 into Eq. 3.53 yields

$$\begin{aligned} MSE &= E\{|\mathbf{w}^H \mathbf{j}|^2\} \\ &= \mathbf{w}^H \mathbf{R}_j \mathbf{w}. \end{aligned} \tag{3.54}$$

Comparison of Eq. 3.52 and Eq. 3.54 indicates that the LCMV criterion is equivalent to a minimum MSE criterion.

Examination of Eq. 3.48 reveals the similarity with the standard Wiener solution. Consider the auto-covariance of $\mathbf{x}(n)$ in Fig. 3.2,

$$\mathbf{R}_x = E\{\mathbf{x}\mathbf{x}^H\} = \mathbf{C}_a^H \mathbf{R}_u \mathbf{C}_a, \tag{3.55}$$

because $\mathbf{x}(n) = \mathbf{C}_a^H \mathbf{u}(n)$.

Now, consider the cross covariance of the signals $\mathbf{x}(n)$ and $q(n)$,

$$\begin{aligned} \mathbf{r}_{xq} &= E\{\mathbf{x}(n)q(n)^H\} && (3.56) \\ &= E\{\mathbf{C}_a^H \mathbf{u}(n)\mathbf{u}^H(n)\mathbf{w}_q\} && (3.57) \\ &= \mathbf{C}_a^H \mathbf{R}_u \mathbf{w}_q. && (3.58) \end{aligned}$$

Comparing Eq. 3.55 and Eq. 3.58 with Eq. 3.48 , we can rewrite Eq. 3.48 as,

$$\mathbf{w}_a = \mathbf{R}_x^{-1} \mathbf{R}_u \mathbf{r}_{xq}, \tag{3.59}$$

which shows the similarity between the standard Wiener solution and the solution implemented with a GSC.

3.3.6 Summary. A beamformer forms a weighted combination of the outputs of spatially separate antennas in order to separate propagating signals that originate from different locations. The weights determine the spatial and temporal filtering characteristics of the beamformer. In an adaptive beamformer the weights are adjusted in response to the data received at the antenna for the purpose of optimizing the beamformer's response. A common criterion for optimizing the weights is minimization of beamformer output power or variance. The goal of minimizing output power is to minimize the contributions of jammer to the output. The LCMV approach minimizes output power subject to a set of linear constraints on the weight vector. These constraints are

used to control the response of the beamformer in the direction of the desired signal to prevent the weights from cancelling the desired signal.

The GSC separates the weight vector into constrained and unconstrained components. The unconstrained components represent the beamformer's adaptive degrees of freedom and are adjusted using standard adaptive algorithm. In order to suppress the jammer signal from different incoming direction, the optimum weight vector and LMS estimate of weight vector were calculated (Eq. 3.48 and Eq. 3.44).

3.4 Adaptive Beamforming in the Presence of Correlated Signals

3.4.1 Introduction. The behavior of adaptive arrays when the interference(s) is correlated with the desired signal is of concern in some environments. We will call two signals fully correlated if one is a scaled, delayed replica of the other. Correlation can destroy the performance of a constrained adaptive array through two effects: 1) the beamformer fails to form deep nulls in the directions of the correlated interferences (Reddy et al, 1987) and 2) the desired signal can be partially or completely cancelled (Widrow et al, 1982). This problem can be overcome by a technique called *spatial smoothing* which modulates the interference in a way that will reduce the correlation with the desired signal. A method of combining spatial smoothing with LMS algorithm will be illustrated.

3.4.2 Analysis of the Decorrelation Effect of Spatial Smoothing. In the GSC depicted in Fig. 3.2, the weights $\mathbf{w}_q$ passes the desired signal through the upper branch while the matrix $\mathbf{C}_a$ blocks it from the lower branch. If however the desired signal is correlated with an interference, the signals in the lower branch of the GSC structure can be used to cancel the desired signal in the upper branch. This is because the interference is a version of the desired signal that is not removed from the lower branch by the spatial filter $\mathbf{C}_a$.

Let $\mathbf{u}(n)$ be the simultaneously sampled vector (*snapshot*) of array signals.

$$\mathbf{u}(n) = [\mathbf{u}_0^H(n), \quad \mathbf{u}_1^H(n), \quad \cdots, \quad \mathbf{u}_{L-1}^H(n)]^H. \tag{3.60}$$

where

$$\mathbf{u}_i^H(n) = [u_{i\times M}(n), \quad u_{i\times M+1}(n), \quad \cdots, \quad u_{i\times M+M-1}(n)], \qquad 0 \le i \le L-1. \tag{3.61}$$

Let the dimension of $\mathbf{u}(n)$ be N where $N = M$ in the narrowband case (Eq. 3.12) and $N = M \times L$ in the wideband case (Eq. 3.13). In Eq. 3.60, $\mathbf{u}$(n) is $N \times 1$ with element,

$$u_i(n) = u[nT_s - mod(i-1, M)T_p - INT(\frac{i-1}{M})T_o], \qquad 1 \le i \le N, \tag{3.62}$$

where *mod* stands for modulo and INT is integer. T_s is sampling time and T_p represents the time delay due to propagation and the delay time T_o of each tap in the TDL antenna array is determined by

$$T_o = \frac{1}{R_s} \tag{3.63}$$

where R_s is the sampling frequency of the arriving signal.

To simplify our work we restrict our analysis to the case of two signals. One of these is the desired signal, and the other is a correlated interference. In Eq. 3.62, $\mathbf{u}(n)$ represents the desired signal when T_p is T_d and interference signal when T_p is T_j.

The basic concept of spatial smoothing is as follows. Assume that the uniform linear array of M sensors is extended with additional sensors and the extended array is grouped into sub-arrays of size M. The first sub-array is formed from the sensors $1, \cdots, M$, and the second sub-array is formed from the sensors $2, \cdots, M+1$, and so on. Let us denote the vector of received signals at

the kth sub-array by $\mathbf{u}^k$. The kth sub array and the i th element of the input vector is,

$$u_i^k(n) = u[nT_s - mod(i+k-1, M+k)T_p + INT(\frac{i-1}{M+k})T_o], \qquad 1 \le i \le N, \qquad (3.64)$$

where the superscript indicates the kth subarray and the subscript indicates the ith element of the input vector. The array covariance matrix of the kth sub-array is then given by

$$\mathbf{R}^k = E\{(\mathbf{u}^k)(\mathbf{u}^k)^H\} \qquad (3.65)$$

We define the spatially smoothing covariance matrix with K number of smoothing steps as

$$\hat{\mathbf{R}} = \frac{1}{K}\sum_{k=1}^{K}\mathbf{R}^k \qquad (3.66)$$

Combining Eq. 3.65 and Eq. 3.66, we obtain

$$\hat{\mathbf{R}} = \frac{1}{K}\sum_{k=1}^{K}E\{(\mathbf{u}^k)(\mathbf{u}^k)^H\} \qquad (3.67)$$

where $\mathbf{u}^k(n)$ is composed of desired signal and interference signal in the kth subarray. Hence, we have

$$\begin{aligned}
\hat{\mathbf{R}} &= \frac{1}{K}\sum_{k=1}^{K}E\{[\mathbf{u}_d^k + \mathbf{u}_j^k][\mathbf{u}_d^k + \mathbf{u}_j^k]^H\} && (3.68)\\
&= \frac{1}{K}\sum_{k=1}^{K}[\mathbf{R}_s^k + \mathbf{R}_j^k + E[(\mathbf{u}_d^k)(\mathbf{u}_j^k)^H] + E[(\mathbf{u}_j^k)(\mathbf{u}_d^k)^H] && (3.69)\\
&= \hat{\mathbf{R}}_s + \hat{\mathbf{R}}_j + \hat{\mathbf{R}}_{sj} + \hat{\mathbf{R}}_{js}, && (3.70)
\end{aligned}$$

where $\hat{\mathbf{R}}_s$ is the autocorrelation of desired signal and $\hat{\mathbf{R}}_j$ is the autocorrelation of jamming signal, and $\hat{\mathbf{R}}_{sj}$ is crosscorrelation between the desired signal and jamming signal in the kth sub-array.

We now study how progressive spatial smoothing reduces the crosscorrelation between all the incident wavefronts, and hence between the desired signal and the other interference wavefronts, and therefore impacts interferences cancellation. If we assume the incident wavefronts are frequency hopped signal, we can write,

$$\mathbf{u}(n) = u(n)\mathbf{e}(h), \qquad T_{h-1} \leq n \leq T_h, \tag{3.71}$$

where the signal arrival vector, $\mathbf{e}(h)$, is $N \times 1$ with element i,

$$e_i(h) = \exp[-j\{mod(i-1, M)\phi_p(h) + INT(\frac{i-1}{M}\phi_p^o(h)\}], \qquad 1 \leq i \leq N. \tag{3.72}$$

Here $\phi_p(h)$ is changed to $\phi_d(h)$ for the desired signal interelement phase shift during hop h and ϕ_j for the interference signal interelement phase shift during hop j, i.e,

$$\begin{aligned} \phi_d(h) &= \omega_h T_d \\ \phi_j(h) &= \omega_j T_j, \end{aligned}$$

where ω_h and ω_j is the desired signal and jamming signal hopping frequencies respectively. Therefore, $\mathbf{e}_d(h)$ represents the desired signal and $\mathbf{e}_j(h)$ does the jamming signal. Also $\phi_p^o(h)$ is the phase shift by delay time T_o, so,

$$\begin{aligned} \phi_d^o(h) &= \omega_h T_o \\ \phi_j^o(h) &= \omega_j T_o. \end{aligned}$$

In Eq. 3.70, the first term $\mathbf{R}_s$ is

$$\hat{\mathbf{R}}_s = \frac{1}{K}\sum_{k=0}^{K} E\{(\mathbf{u}_d^k)(\mathbf{u}_d^k)^H\}$$

$$
\begin{aligned}
&= \frac{1}{K}\sum_{k=0}^{K} E\{u_d u_d^H\} E\{(\mathrm{e}_d^k(h))(\mathrm{e}_d^k(h))^H\} \\
&= \mathbf{R}_s \frac{1}{K}\sum_{k=0}^{K} \exp[-j\{mod(i+k-1, M+k)(\phi_d - \phi_d) + INT((i-1)/(M+k))(\phi_d^o - \phi_d^o)\}] \\
&= \mathbf{R}_s,
\end{aligned}
$$

because ϕ_d and ϕ_d^o cancel out causing the exponential terms to zero. Thus exponential becomes equal to one and thus the sum adds to K. Also $\hat{\mathbf{R}}_j = \mathbf{R}_j$. Therefore Eq. 3.70 is

$$
\begin{aligned}
\hat{\mathbf{R}}_s &= \mathbf{R}_s + \mathbf{R}_j \\
&+ \mathbf{R}_{sj} \frac{1}{K}\sum_{k=1}^{K} \exp[-j\{mod(i+k-1, M+k)(\phi_d - \phi_j) + INT((i-1)/(M+k))(\phi_d^o - \phi_j^o)\}] \\
&+ \mathbf{R}_{js} \frac{1}{K}\sum_{k=1}^{K} \exp[-j\{mod(i+k-1, M+k)(\phi_j - \phi_d) + INT((i-1)/(M+k))(\phi_j^o - \phi_d^o)\}].
\end{aligned}
$$

The crosscorrelation parts (the third and fourth parts of above equation) go to zero as the number of smoothing steps, K, goes to infinity. Therefore the signals are progressively decorrelated. The rate which the cross-correlation part approaches zero depends on the hopping frequency and propagation delay (Reddy et al, 1987).

The smoothing covariance matrix (Eq. 3.66) is used to calculate the weight vector $\mathbf{w}_a$ in the GSC, as Eq. 3.44

$$
\mathbf{w}_a(n+1) = \mathbf{w}_a(n) + \mu \mathbf{C}_a^H \hat{\mathbf{R}}(\mathbf{w}_q - \mathbf{C}_a \mathbf{w}_a(n)). \tag{3.73}
$$

3.4.3 Summary. A jammer that is correlated with the desired signal arises due to multipath propagation or intelligent jamming and creates a special problem for conventional adaptive beamforming. The goal of this section was to illustrate how spatial smoothing combined with a LMS adaptation of array weights can remove correlated interference in a GSC. The crosscorrelation between desired signal and jammer signal goes to zero as the number of smoothing steps, K, goes to infinity.

3.5 Conclusion

This chapter illustrated the theory of adaptive signal processing. The temporal and spatial filters mathematical formulations and procedures for their solution are indeed similar, even though they are used in different application areas. Adaptive temporal filter converges to the optimum Wiener solution in a stationary environment. The adaptive beamformer as the spatial filter forms a weighted combination of the outputs of spatially separated antennas in order to suppress propagating signals that originate from different locations. The LCMV-GSC beamformer is used, which minimize the output power with related to the undesired signals. The adaptive arrays when the interference(s) is correlated with the desired signal were totally destroyed. As the solution, Section 3.4 suggested the *spatial smoothing technique* to reduce the crosscorrelation between the desired signal and the jamming signal. The next chapter will simulate the jamming suppression in the several cases.

IV. Simulation

This chapter considers the simulation of jamming suppression in several cases. A LAS antenna array has just M antenna elements [Fig. 1.1] while TDL antenna array has L delayed taps in each of the mth antenna element channel [Fig. 2.4]. Section 4.1 compares the performance of wideband interference suppression in these two different antenna arrays. Next section 4.2 presents two techniques in the frequency hopped environment. The first technique is the conventional method in which only the center frequency of the desired signal is used in the constraint matrix (Eq. 3.19). The second one uses each hopping frequency of the desired signal. For all of the above cases, we assume that the desired signal and the jamming signals are uncorrelated. In section 4.3, we investigate the case when the desired signal and jammer signals are correlated. Finally the results of using an adaptive filter in the time domain for narrowband jamming signals suppression is presented.

4.1 Wideband Jamming Suppression in Antenna Arrays,

4.1.1 LAS Antenna Array and Frequency Characteristics. As described in Section 3.3.2, the signal output of a LAS antenna array with M antennas is

$$y(n) = \mathbf{w}^H \mathbf{u}(n). \tag{4.1}$$

where $y(n)$ is the output of antenna array, and $\mathbf{w}$ is weight vector and $\mathbf{u}(n)$ is input signal vector,

$$\begin{aligned} \mathbf{w} &= [w_1, w_2, \cdots, w_M] \\ \mathbf{u}(n) &= [u_1(n), u_2(n), \cdots u_M(n)] \\ u_i(n) &= u[nT_s - mod(i-1, M)T_p], \qquad 1 \le i \le M \end{aligned}$$

where $T_p = \frac{d}{c}\sin(\theta_p)$ is the interelement propagation delay : θ_p is the direction of the incident signal. The subscript d for the desired signal and j for the jammer signal, d is the antenna interelement space which is a half wavelength at the center frequency. Thus

$$\begin{aligned} T_p &= \frac{d}{c}\sin\theta_p \\ &= \frac{\lambda}{2c}\sin\theta_p \\ &= \frac{1}{2f_c}\sin\theta_p. \end{aligned}$$

The signal vector, $\mathbf{u}(n)$ can be written as

$$\mathbf{u}(n) = \mathbf{u}_d(n) + \mathbf{u}_j(n), \tag{4.2}$$

where $\mathbf{u}_d(n)$ and $\mathbf{u}_j(n)$ are vectors containing the desired and interference signals respectively. $\mathbf{u}_d$ and $\mathbf{u}_j(n)$ are assumed to be uncorrelated.

To calculate the weight coefficient of the LAS antenna array, a linear constraint minimum variance generalized sidelobe canceller (LCMV-GSC) beamformer is used as described in Section 3.3.5. The desired signal direction gain-only constraint equation is expressed as,

$$\mathbf{C}^H\mathbf{w} = \mathbf{f}, \tag{4.3}$$

where $\mathbf{C}$ is the constraint matrix, $\mathbf{C} = \mathbf{d}(\theta_d, \omega_c)$ and $\mathbf{f}$ is the response vector, $\mathbf{f} = 1$.

$$\mathbf{d}(\theta_d, \omega_c) = [1, \quad e^{j\omega_c T_d}, \quad e^{j2\omega_c T_d}, \quad \cdots, \quad e^{j(M-1)\omega_c T_d}]^H, \tag{4.4}$$

where θ_d is the incident direction, measured with respect to the boresight (i.e., the normal to the array), ω_c is the center frequency of the desired signal.

The non-adaptive beamformer component in the generalized sidelobe canceller (GSC) is rep-

resented by, as in Eq. 3.36

$$\mathbf{w}_q = \mathbf{C}\mathbf{q} = \mathbf{C}(\mathbf{C}^H\mathbf{C})^{-1}\mathbf{f}. \tag{4.5}$$

As shown in Fig. 3.2, the weight can be expressed by Eq. 3.37,

$$\mathbf{w} = \mathbf{w}_q - \mathbf{C}_a\mathbf{w}_a, \tag{4.6}$$

where the adaptive beamformer component in the GSC is updated as in Eq. 3.44,

$$\begin{aligned} \mathbf{w}_a(n+1) &= \mathbf{w}_a(n) + \mu\mathbf{x}(n)e^*(n) \\ &= \mathbf{w}_a(n) + \mu\mathbf{C}_a^H\mathbf{u}(n)(\mathbf{w}_q^H\mathbf{u}(n) - \mathbf{w}_a^H\mathbf{C}_a^H\mathbf{u}(n))^* \\ &= \mathbf{w}_a(n) + \mu\mathbf{C}_a^H\mathbf{u}(n)\mathbf{u}(n)^H(\mathbf{w}_q - \mathbf{C}_a\mathbf{w}_a(n)) \end{aligned} \tag{4.7}$$

and optimum weight vector of the adaptive beamformer component is as in Eq. 3.48,

$$\mathbf{w}_a = (\mathbf{C}_a^H\mathbf{R}_u\mathbf{C}_a)^{-1}\mathbf{C}_a^H\mathbf{R}_u\mathbf{w}_q \tag{4.8}$$

The output frequency transfer function is (Wang et al, 1993)

$$H(\omega) = \sum_{k=0}^{M-1} w_m e^{-jw[(m-1)T_p]} \tag{4.9}$$

where T_p is the propagation delay time between the elements for the arriving wave. The propagation delay time T_p might be changed to T_d for the desired signal and to T_j for the jammer signal. Hence the output frequency transfer function of the LAS antenna array for the desired and jamming signals can be expressed in a similar form.

If the direction of the desired signal is known, the weight coefficients w_k for the antenna array are derived by means of the LMS adaptive algorithm as in Eq. 4.6 and Eq. 4.7. As numerical

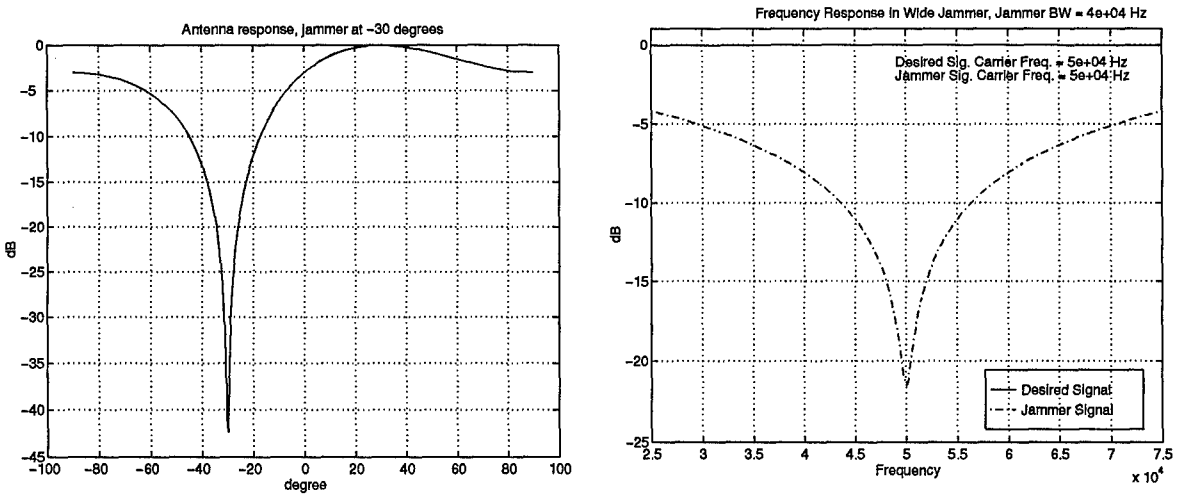

(a) (b)

Figure 4.1 (a) Antenna Array Pattern, (b) Frequency Characteristic in the LAS Antenna Array

examples, the antenna pattern and the frequency characteristics of the LAS antenna array with two elements ($M = 2$) are shown in Fig. 4.1 for two arriving signals ($i = 2$). In the antenna pattern, the desired signal incident at an angle of 30^o from boresight is passed undistorted, while the jamming signal at an angle of -30^o is rejected. This is more clear in the frequency characteristics graph of a Fig. 4.1. The solid line is the desired signal normalized to zero. This signal passes through the antenna array whereas the dashed line shows an attenuation of the jamming signal. This figure also shows that the possible blocking bandwidths of the jamming signal are confined to narrow bandwidths.

4.1.2 TDL Antenna Array and Frequency Characteristics, Fig. 2.4 shows the configuration of the TDL(tapped delay line) antenna array in which several tap weights are provided for each antenna channel. In adaptive beamforming for narrowband jammers, the directivity is constructed by means of the spatial correlation characteristics of the signals between elements. In the case of the TDL array, in addition to the capability of forming an identical directivity, the temporal correlation characteristics of the signals among the taps can be used in such a way as to improve the frequency characteristics for the arriving signal with a broad bandwidth.

The signal output of a TDL linear array with M antennas, each followed by a tapped delay-line with L taps, is

$$y(n) = \mathbf{w}^H \mathbf{u}(n). \tag{4.10}$$

where

$$\begin{aligned} \mathbf{w} &= [w_1, w_2, \cdots, w_{ML}] \\ \mathbf{u}(n) &= [u_1(n), u_2(n), \cdots u_{ML}(n)] \\ u_i(n) &= u[nT_s - mod(i-1, M)T_p - INT(\frac{i-1}{M})T_o] \qquad 1 \le i \le ML \end{aligned}$$

and where T_p is the propagation delay time between the elements for the arriving wave. The delay time T_o of each tap in the TDL antenna array is determined by

$$T_o = \frac{1}{R_s}, \tag{4.11}$$

where R_s is the sampling frequency of the arriving signal.

In the constraint equation for the LCMV beamformer as in Eq. 3.19, the desired signal direction gain-only constraint is,

$$\mathbf{f} = [1, 0 \ldots, 0]^T \tag{4.12}$$

$$\mathbf{C} = \begin{pmatrix} \mathbf{d}(\theta_d, \omega_c) & 0_M & \ldots & 0_M \\ 0_M & \mathbf{d}(\theta_d, \omega_c) & \ldots & 0_M \\ \vdots & \vdots & \ddots & \vdots \\ 0_M & 0_M & \ldots & \mathbf{d}(\theta_d, \omega_c) \end{pmatrix} \tag{4.13}$$

where $\mathbf{d}(\theta_d, \omega_c)$ is $M \times 1$, where θ_d is the direction, measured with respect to the boresight, ω_c is the center frequency of the desired signal, and is expressed as,

$$\mathbf{d}(\theta_d, \omega_c) = [1, \quad e^{-j\omega_c T_d}, \quad e^{-j2\omega_c T_d}, \quad \cdots, \quad e^{-j(M-1)\omega_c T_d}]^H, \tag{4.14}$$

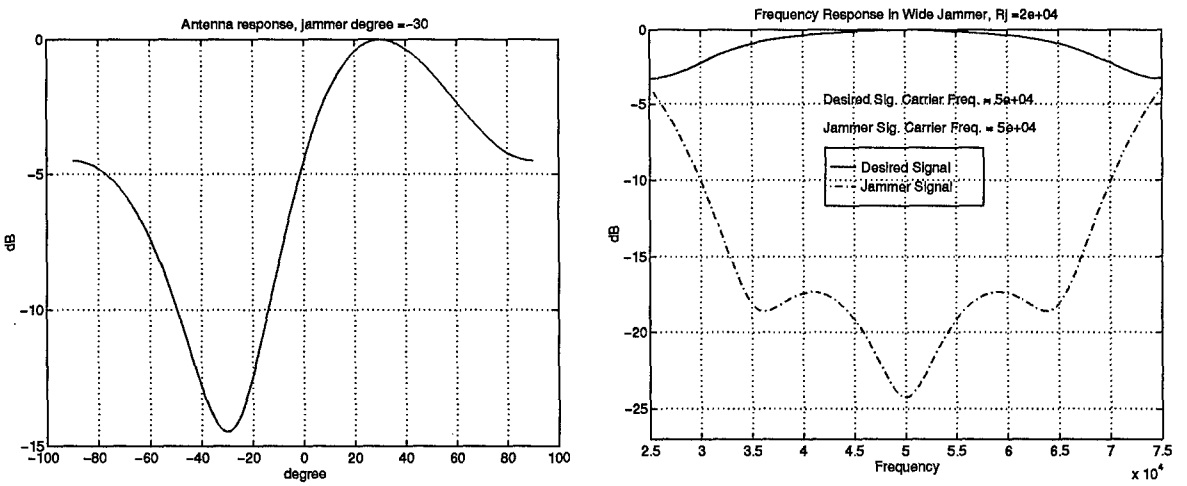

(a) (b)

Figure 4.2 (a) Antenna Array Pattern, (b) Frequency Characteristic in the TDL Antenna Array

and the column vectors 0_M contain M zeros. The L-dimensional gain vector $\mathbf{f}$ describes the frequency response of the beamformer to a signal impinging on the array from the desired look direction . Thus the constraint matrix $\mathbf{C}$ is $ML \times L$ dimensional (Buckley and Griffiths, 1988).

Using the weight coefficient which is updated by Eq. 4.6 and Eq. 4.7, the output frequency transfer function is given by

$$H(\omega) = \sum_{m=1}^{M} \sum_{l=1}^{L} w_{m,l} e^{-j\omega[(m-1)T_p + (l-1)T_o]}. \tag{4.15}$$

The frequency characteristics of the TDL antenna array output with two elements each by having five delay taps are shown in Fig. 4.2(b) for the two arriving signals. The antenna array pattern of the computed TDL antenna array is similar to those in Fig. 4.1(a). The output frequency characteristics pass the desired signal while the frequency components of the wideband interference signal within the bandwidth can be sufficiently suppressed. As a result, the TDL adaptive antenna array is more effective for the suppression of wideband interferences than the LAS antenna array.

Item	Desired Signal	Jamming Signal
Direction at Arrival	30^o	-30^o
Carrier Frequency	$15 \times 10^4(Hz)$	$15 \times 10^4(Hz)$
Bandwidth	$6 \times 10^3(Hz)$	6×10^3
Sampling Frequency	12×10^6 Hz	
No. of TDL array elements	8	
No. of TDL tap elements	10, 20	
TDL array tap delay	1/Rs	

Table 4.1 Specification for First Computer Simulation

4.1.3 Comparison of Two Antennas. In the previous section, the output frequency characteristics of the LAS and TDL adaptive antenna array were studied. In this section, the performance of two antenna arrays is compared using output signal to jammer ratio (SJR) in the presence of wideband jammers. The wideband signals shown in Table 4.1 were used for this simulation. Their fractional bandwidth is a $\frac{6}{150} = 0.04$. Fractional bandwidth larger than 0.02 are defined as wideband signals [section 3.1.3].

The performance of this system is demonstrated by exploring the input and output SJR and improvement defined as,

$$SJR_o = \frac{S_o}{J_o}$$

$$SJR_i = \frac{S_i}{J_i} \tag{4.16}$$

$$IMP = \frac{SJR_o}{SJR_i} \tag{4.17}$$

where S_i and S_o is the desired signal input and output power, and J_i and J_o is the jamming signal power, respectively.

The LMS weight estimate is updated at each time n by Eq. 4.6 and Eq. 4.7. Fig. 4.3 shows the IMP of the LAS and TDL antenna array as the function of iteration. Both systems have a good convergence characteristic. IMP of the TDL antenna array converges to higher value than IMP of the LAS antenna array. In order to see this more clearly, the IMP is separated into the

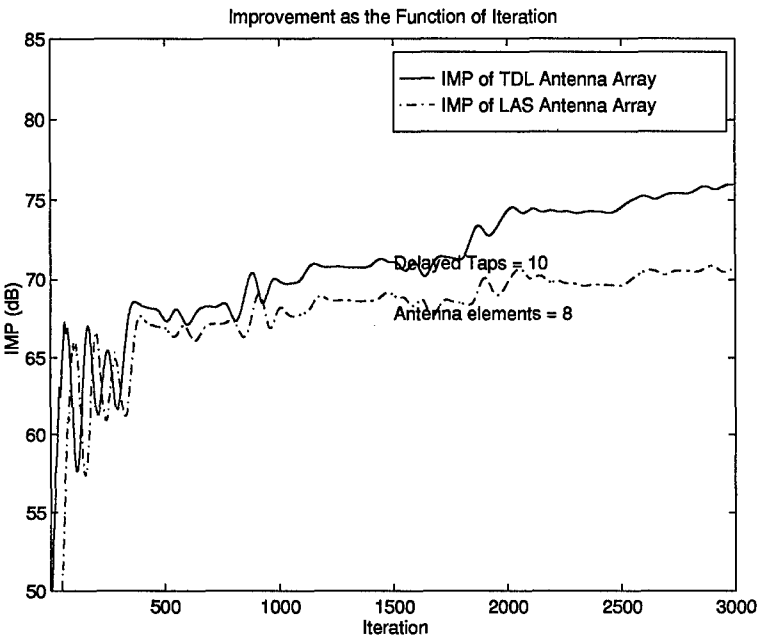

Figure 4.3 IMP in LAS and TDL Antenna Array using LMS Weight Estimate

desired signal power (S_o and S_i) and the jamming signal power (J_o and J_i). Fig. 4.4(a) shows the desired signal power variation as a function of iteration. The solid line is the desired signal input power (S_i), and the dashed line is the desired signal output power (S_o) of the LAS antenna array. The dotted line is S_o of the TDL antenna array. The desired signal output power (S_o) is close to the signal input power (S_i) in both antennas while the jammer signal is suppressed significantly [Fig. 4.4(b)]. In Fig. 4.4(b), the dotted line shows the jamming signal output power in the LAS antenna array while the dashed line shows it in the TDL antenna array. As a result, Fig. 4.4(b) shows that the jamming signal is suppressed more efficiently in the TDL antenna array than in the LAS antenna array as much as 10dB. Therefore, we can prove the TDL antenna array is more efficient than the LAS antenna array for wideband jammers suppression. Fig. 4.4(c) and Fig. 4.4(d) show the same effect as Fig 4.1(b) and Fig 4.2(b).

The next experiment shows the effect of increasing the delayed taps from 10 to 20 for a fixed number of antenna elements (M=8). As expected, the performance of the TDL antenna array is improved by increasing the delay taps from 10 to 20 [Fig. 4.5]. The desired signal power (S_o) is not

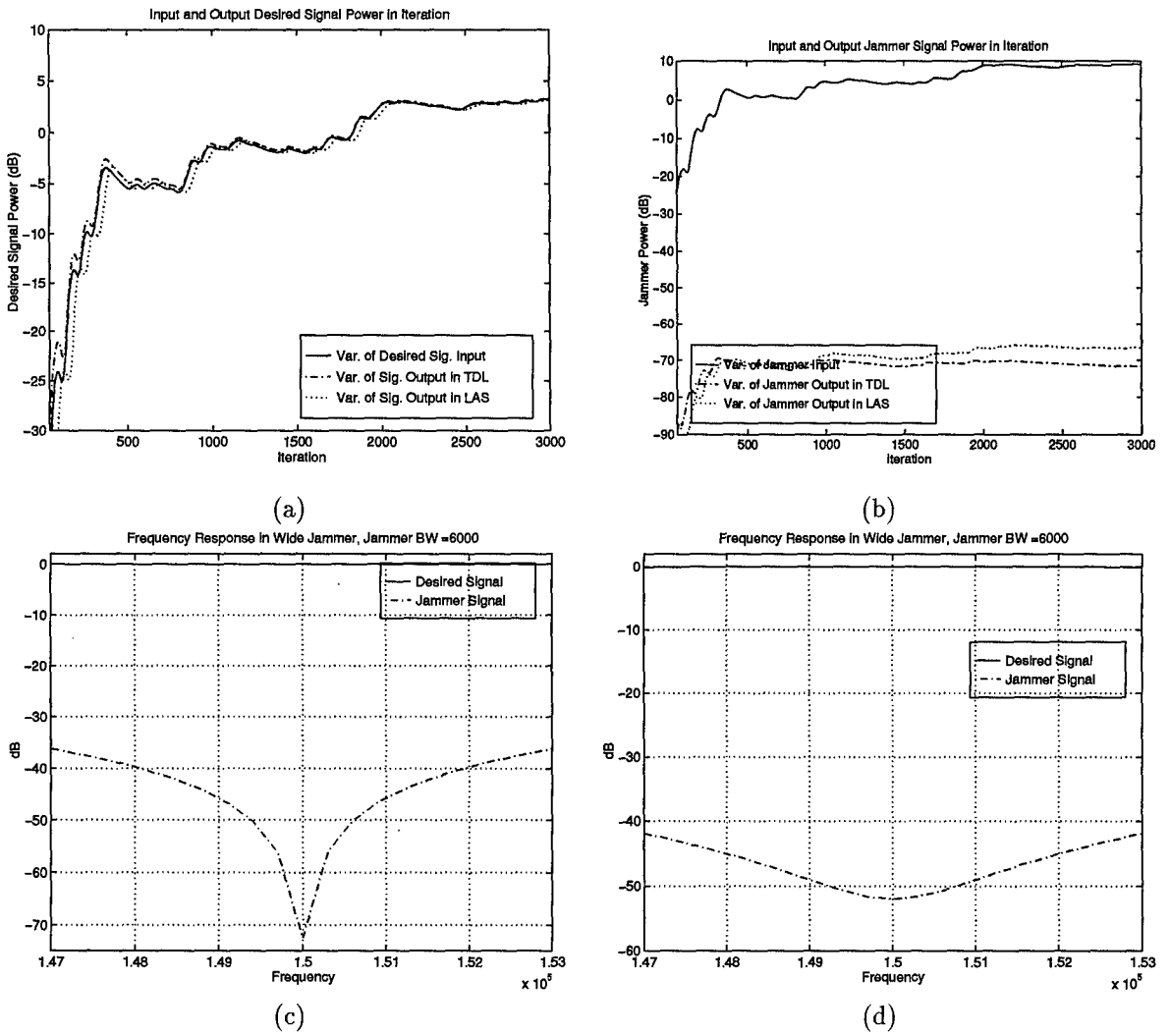

Figure 4.4 Input and Output Power of TDL and LAS Antenna Arrays (a) Desired Signal Part, (b) Jamming Signal Part, Frequency Characteristics of (c) LAS Antenna Array and (d) TDL Antenna Array Respectively

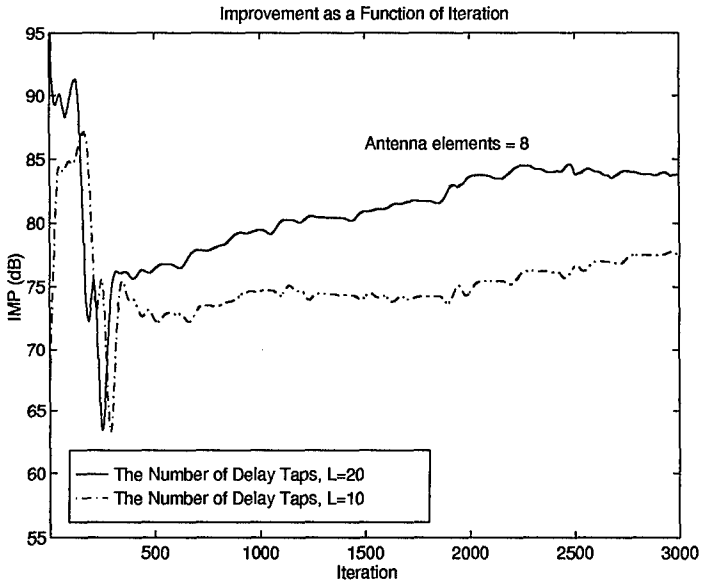

Figure 4.5 The Comparison Between $K = 10$ and $K = 20$ in the TDL Antenna Array

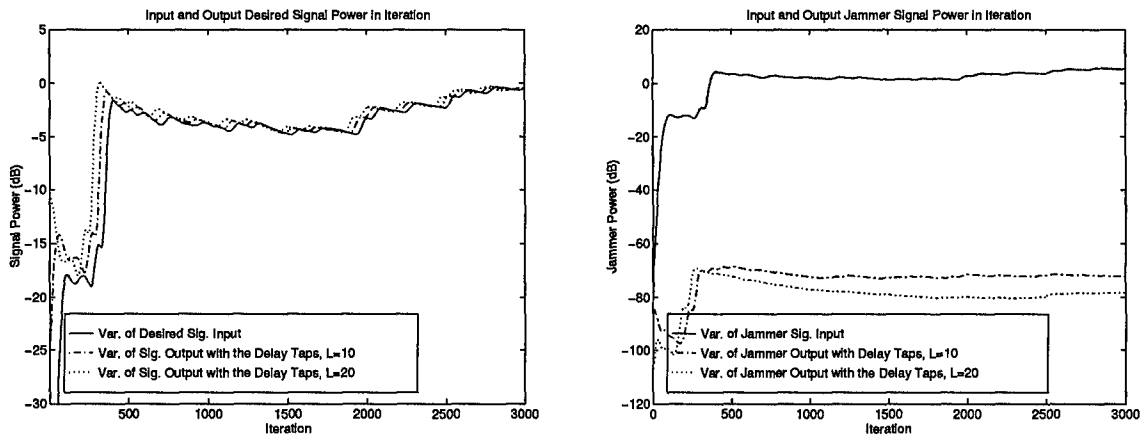

(a) (b)

Figure 4.6 The Comparison Between $K = 10$ and $K = 20$ in the TDL Antenna Array (a) The Desired Signal Part, (b) The Jamming Signal Part

Item	Desired Signal	Jamming Signal
Direction at Arrival	30^o	-30^o
Carrier Frequency	$15 \times 10^4(Hz)$	$15 \times 10^4(Hz)$
Bandwidth	$3 \times 10^4(Hz)$	3×10^4
Sampling Frequency	12×10^6 Hz	

Table 4.2 Specification for Second Computer Simulation

changed much when compared to the input signal power (S_i) [Fig. 4.6(a)]. On the other hand, as the number of delay taps increases, the jamming signal power is reduced significantly [Fig. 4.6(b)].

The next simulation considers the changes when the fraction bandwidth increased form 0.04 to 0.2 as shown in Table 4.2. This means that the BW of signals in specification of computer simulation is changed from 6×10^3 to 3×10^4. Fig. 4.7 still shows the TDL antenna array is more effective in suppression of the jamming signal than the LAS antenna array. If we see Fig. 4.8(a), however, there are difference from Fig. 4.6(a). The desired signal output power (S_o) is decreased in the both antenna arrays. This is due to the fact that the LCMV-GSC beamformer constrained the direction and center frequency of the desired signal using a constraint matrix. If the input signal is narrowband, there is no distortion of the desired signal. In this experiment, however, the input signal has extremely wide bandwidth (fractional BW = 0.2). As the signal bandwidth increases, the distortions are increased in the desired signal except the center frequency used in the constraint matrix. As you see Fig. 4.4 (c) and (d), the desired signal has unity gain at the center frequency. Other frequencies are attenuated. Thus, if the desired signal has wide bandwidth, this signal is distorted passing the antenna arrays.

Another interesting point in Fig. 4.8(a) is that the desired signal output power (S_o) of the LAS antenna array is slightly higher than the S_o of the TDL antenna array. The phase difference between the weight coefficients depends on the time delay and frequencies of the desired signal. The constraint however fixes the phase with respect to the center frequency and the time delay. Due to difference in phase between the real weights and the constraint, distortion occurs. In the LAS antenna array, only M antenna elements affect the distortion while the distortion is affected

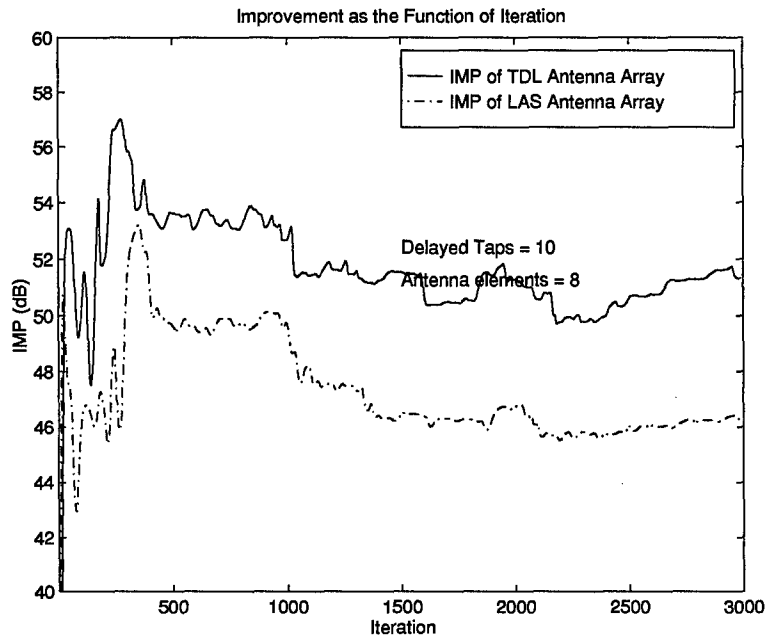

Figure 4.7 IMP in LAS and TDL Antenna Array using LMS Weight Estimate

by not only M antenna elements but also $(M-1)L$ delayed taps in the TDL antenna array.

Fig. 4.8(b) indicates the jamming signal input and output powers as a function of iteration. Both systems show the good convergence for jamming signal suppression. As the number of the iteration increases, the TDL antenna array suppresses the jamming signal more than the LAS antenna array.

The next experiment shows the performance effect by increasing the delayed taps from 10 to 20 in the extreme wideband signals. The IMP of the TDL antenna array decreases even though the number of delayed taps increases, as shown in Fig. 4.9. The reason is that the desired signal distortion was more serious with the larger number of delayed taps [Fig 4.10(a)]. Furthermore the capability of the jamming signal suppression is not even changed [Fig 4.10(b)].

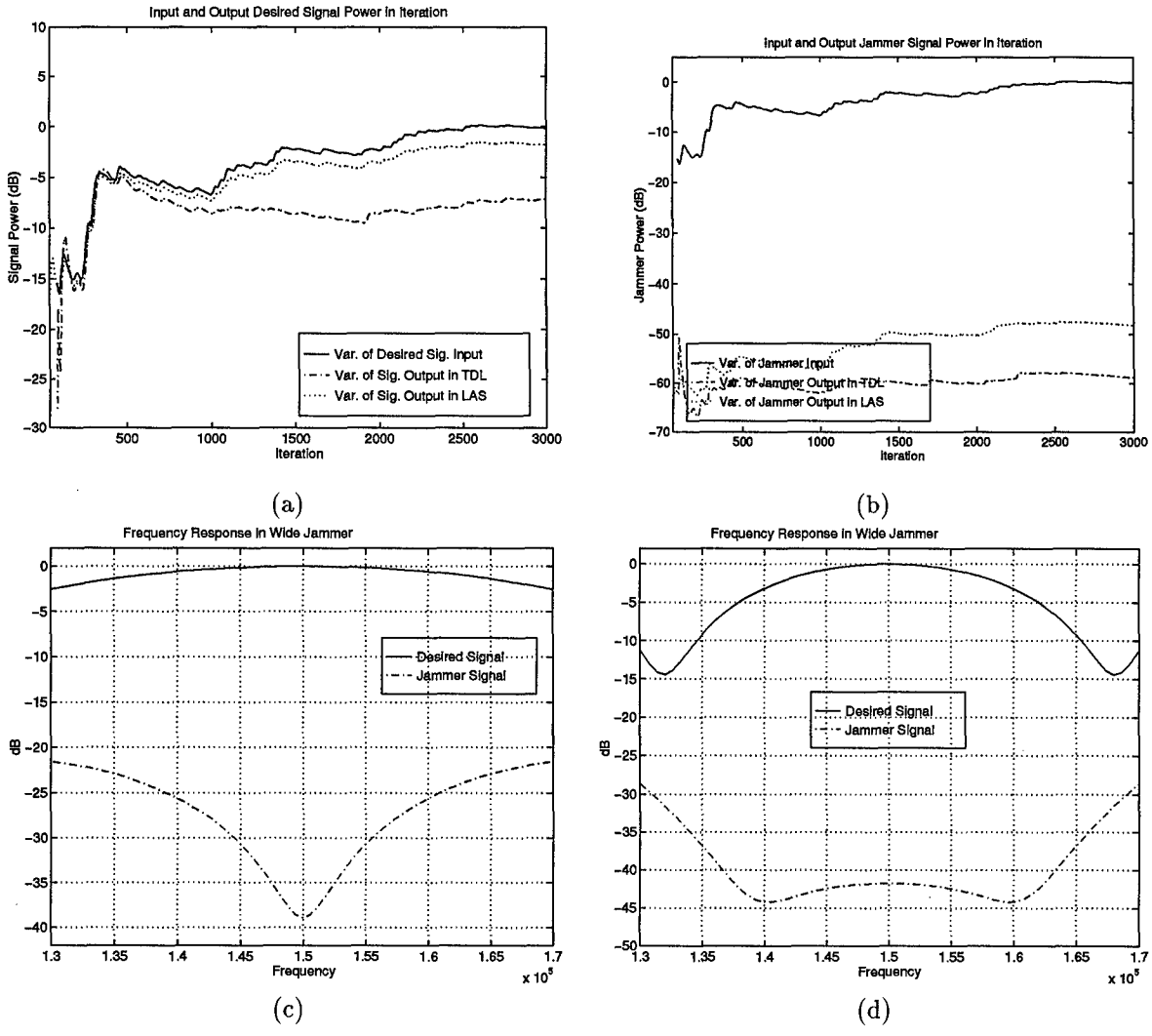

Figure 4.8 Input and Output Power of TDL and LAS Antenna Arrays (a) Desired Signal (b) Jamming Signal, Frequency Characteristics of (c) LAS Antenna Array and (d) TDL Antenna Array Respectively

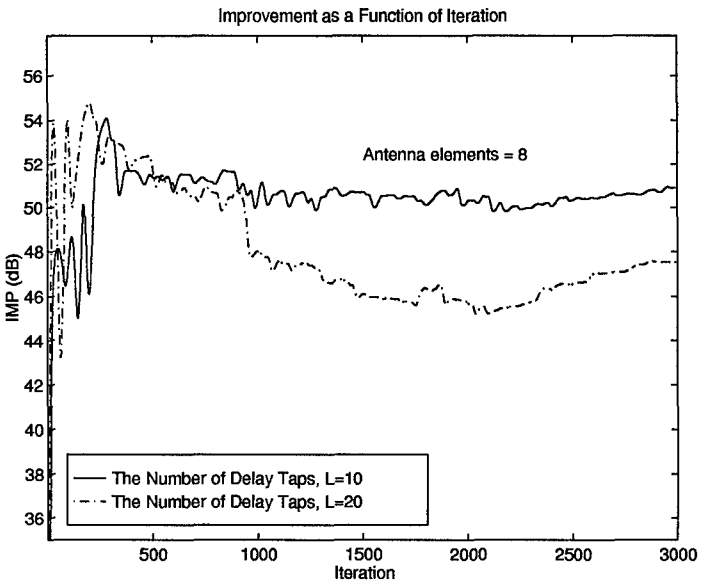

Figure 4.9 The Comparison Between $K = 10$ and $K = 20$ in the TDL Antenna Array

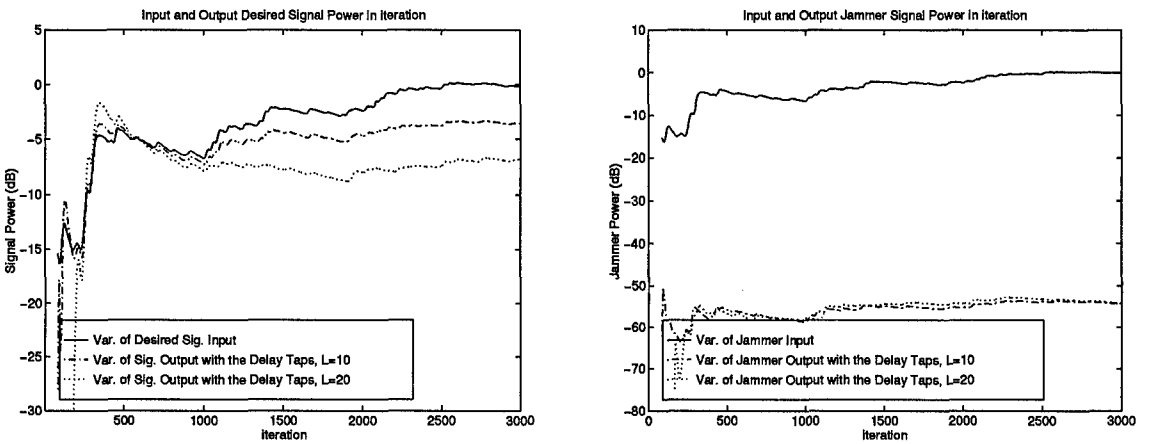

(a) (b)

Figure 4.10 The Comparison Between $K = 10$ and $K = 20$ in the TDL Antenna Array (a) The Desired Signal Part, (b) The Jamming Signal Part

4.2 Jamming Suppression in Frequency-Hopped Environment

This section examines the output SJR performance of adaptive arrays in a Frequency-Hopped (FH) environment. The combined effects of the arrays interference nulling ability and the interference protection of FH signals result in a more robust interference rejection communication system. As concluded in the previous section, the TDL antenna array should be more effective than the LAS antenna array for frequency-hopped jamming signal suppression, because FH signals also have wide bandwidths.

In the next example, two different techniques are used for frequency hopped jamming suppression in the TDL antenna array. The first conventional technique is the same as the method of section 4.1.2, which uses the center frequency in the constraint matrix. The second method uses a hopping frequency in the constraint matrix.

4.2.1 Conventional Technique for Frequency-Hopped Environment. For the experiment, the TDL(tapped delay line) antenna array is used. With M antenna elements spaced a half wavelength apart at the center frequency of the FH band, $\omega_c = 2\pi f_c$. A desired signal is incident on the array from direction θ_d and with hopping frequencies $\omega_h = 2\pi f_h$, and an jamming signal from direction θ_j and at its hopping frequencies $\omega_j = 2\pi f_j$. The input signal vector, $\mathbf{u}(n)$ can be written as,

$$\mathbf{u}(n) = \mathbf{u}_d(n) + \mathbf{u}_j(n), \tag{4.18}$$

where $\mathbf{u}_d(n)$ and $\mathbf{u}_j(n)$ are vectors containing the desired and interference signals respectively. $\mathbf{u}_d$ and $\mathbf{u}_j(n)$ are assumed to be uncorrelated.

The delay time T_o of each tap in the TDL antenna array is determined by

$$T_o = \gamma \frac{1}{4f_c}, \tag{4.19}$$

where f_c is the carrier frequency of the arriving signal. R.T Compton shows the coefficient γ in his journal (Compton, 1988) as

$$\frac{1}{B} < \gamma < \frac{4}{B}, \tag{4.20}$$

where B is determined as the normalized jammer bandwidth, $\frac{BW_j}{f_c}$.

The form of the desired signal vector and interference signal vector are

$$\mathbf{u}(n) = u(n)\mathbf{e}(h), \qquad T_{h-1} \leq n \leq T_h, \tag{4.21}$$

where $T_{h-1} \leq n \leq T_h$ is the time duration of the h^{th} hop interval, and the signal arrival vector is,

$$e_i(h) = \exp[-j\{mod(i-1, M)\phi_p(h) - INT(\frac{i-1}{M})\phi_p^o(h)\}]. \tag{4.22}$$

Here, $\phi_d(h)$ is the desired signal interelement phase shift during hop h and ϕ_j is the interference signal interelement phase shift during hop j, i.e,

$$\begin{aligned} \phi_d(h) &= \omega_h T_d \\ \phi_j(h) &= \omega_j T_j, \end{aligned}$$

and $\phi_p^o(h)$ is the phase shift due to taps delay time T_o, so,

$$\begin{aligned} \phi_d^o(h) &= \omega_h T_o \\ \phi_j^o(h) &= \omega_j T_o. \end{aligned}$$

The constraint matrix and the weight coefficient of the TDL antenna array is the same as the section 4.1.2. The frequency characteristics of the frequency hopped signals and the comparison between the LAS antenna array and the TDL antenna array are very similar to Fig. 4.2 and Fig. 4.3, respectively since frequency hopped signals belong to the wideband signals.

4.2.2 New Technique for Frequency-Hopped Environment. The signal output of the TDL linear array with M antennas, each followed by a tapped delay-line with L taps, is

$$y(n) = \mathbf{w}^H \mathbf{u}, \tag{4.23}$$

where

$$\begin{aligned} \mathbf{w} &= [w_1, w_2, \cdots, w_{ML}] \\ \mathbf{u} &= u(n)\mathbf{e}(h), \qquad\qquad T_{h-1} \leq n \leq T_h. \end{aligned}$$

The signal arrival vector is

$$e_i(h) = \exp[-j\{mod(i-1, M)\phi_p(h) - INT(\frac{i-1}{M})\phi_p^o(h)\}]. \tag{4.24}$$

Here, $\phi_d(h)$ is the desired signal interelement phase shift during hop h, and ϕ_i is the interference signal interelement phase shift. And $\phi_p^o(h)$ is the phase shift due to delay time T_o.

In the constraint equation, the desired signal direction gain-only constraint is,

$$\mathbf{f} = [1, 0 \ldots, 0]^T, \tag{4.25}$$

and

$$\mathbf{C} = \begin{pmatrix} \mathbf{d}(\theta_d, \omega_h) & 0_K & \ldots & 0_M \\ 0_M & \mathbf{d}(\theta_d, \omega_h) & \ldots & 0_M \\ \vdots & \vdots & \ddots & \vdots \\ 0_M & 0_M & \ldots & \mathbf{d}(\theta_d, \omega_h) \end{pmatrix} \tag{4.26}$$

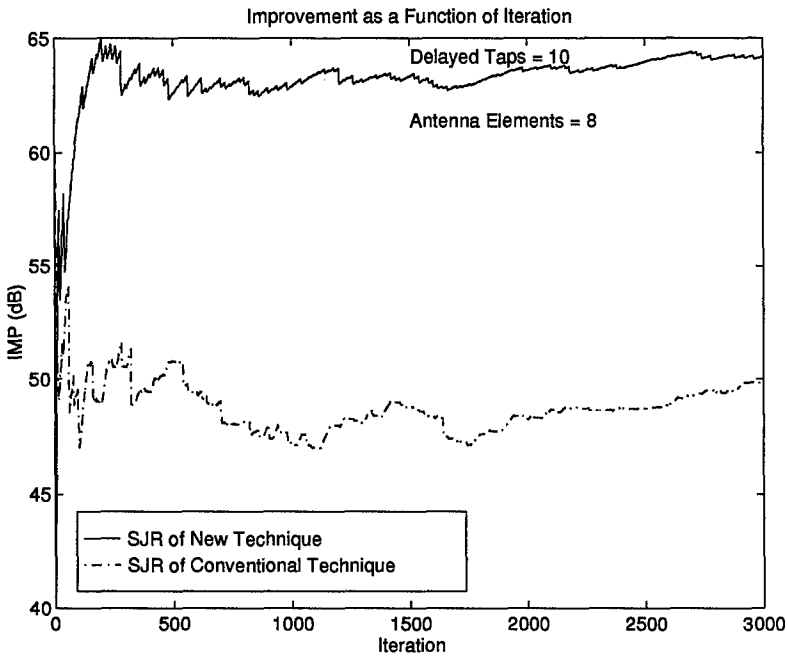

Figure 4.11 Comparison of IMP Between Two Different Techniques

where $\mathbf{d}(\theta_d, \omega_h)$ is $M \times 1$, where θ_d is the direction, measured with respect to the boresight, ω_h is the hopping frequency of the desired signal respectively, and is expressed as

$$\mathbf{d}(\theta_d, \omega_h) = [1, \quad e^{-j\omega_h T_d}, \quad e^{-j2\omega_h T_d}, \quad \cdots, \quad e^{-j(M-1)\omega_h T_d}]^H. \tag{4.27}$$

The difference here compared to the conventional method is that the hopping frequency is used in the constraint matrix instead of the center frequency. The output frequency transfer function remains the same as Eq. 4.15.

4.2.3 Comparison of the Two Techniques. The frequency-hopped signals generated by Table 4.2 are used for this experiment. They are incident into the antenna, each having their own direction. The TDL antenna array weights are updated by the LCMV-GSC algorithm, as described in Eq. 4.6 and Eq. 4.7. Fig. 4.11 shows the IMP of the two techniques for the TDL antenna array.

As a result, IMP of the new technique is higher than IMP of the conventional technique as much as 15dB.

This can be explained in Fig. 4.12. In Fig. 4.12(a), the desired signal output power of the new technique is same as the input power while S_o of the conventional method is reduced. In the constraint matrix, the new technique constrains each hopping frequency, therefore the frequency characteristics of the desired signal attempts to match the hopping frequency. When the hopping frequency of the desired signal is changed, the frequency characteristic of the desired signal has a unity gain at the hopping frequency as shown in Fig. 4.12(c). Therefore, there is no distortion in the desired signal part. On the other hand, in the conventional method, the frequency characteristics of desired signal maintains the center frequency with a unity gain even though the signal frequencies are changed to the other hopping frequencies. Thus there is some distortion at the other hopping frequencies [Fig. 4.12(d)]. Fig. 4.12(b) shows that the jamming suppression capability of the new technique is greater than the conventional technique.

In the new technique, the next experiment investigated the change when the the number of taps increases from 10 to 20. Fig 4.13 shows the IMP for two different numbers of delay taps. Unlike the conventional method, the IMP increases by increasing the number of taps. This occurs because the desired signal power (S_o) is not attenuated while the jamming signal is more suppressed by increasing the number of delay taps (Fig. 4.14(a)(b)).

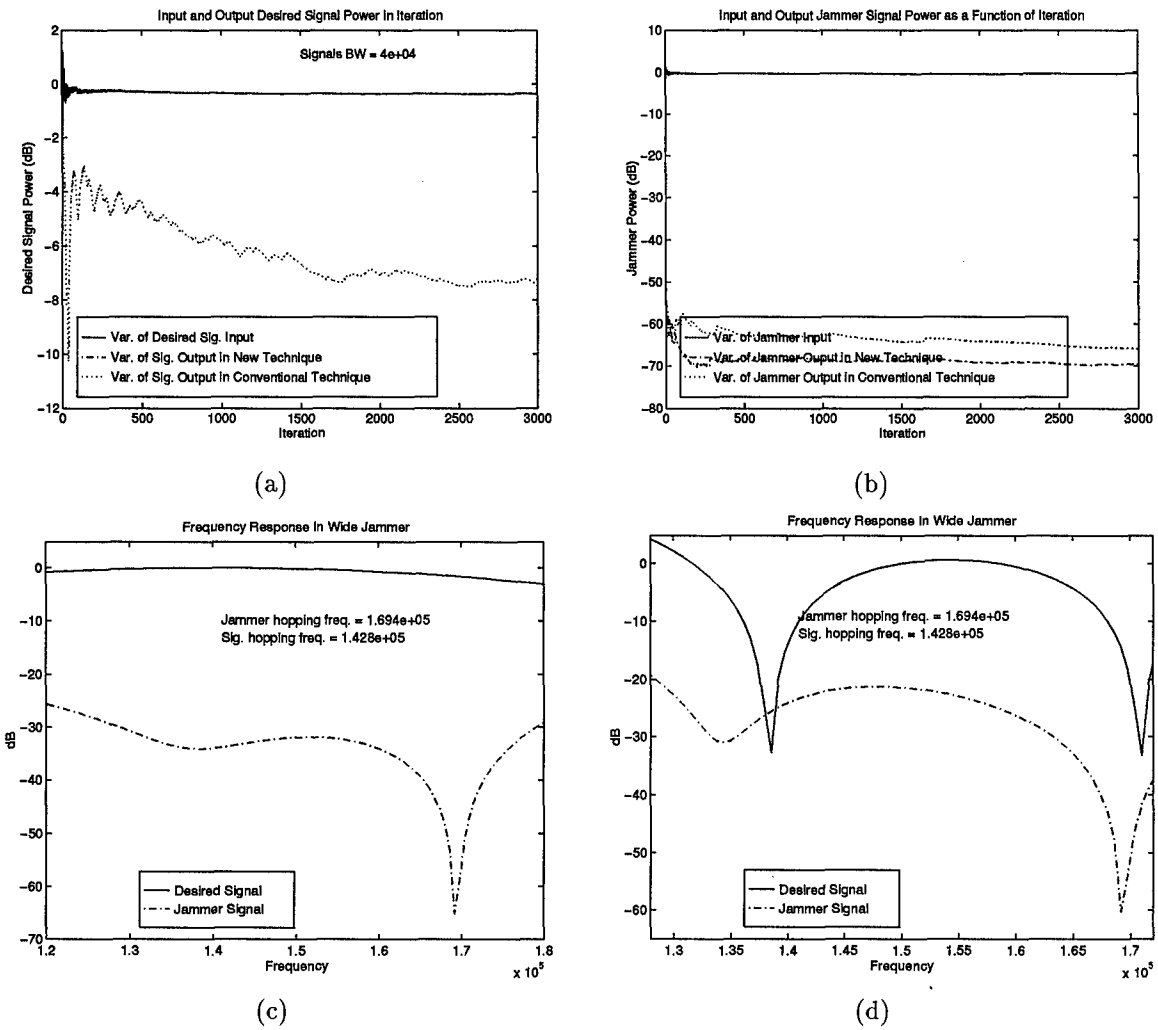

Figure 4.12 Input and Output Power of New and Conventional Technique (a) Desired Signal Part (b) Jamming Signal Part, Frequency Characteristics of (c) New Technique and (d) Conventional Technique Respectively

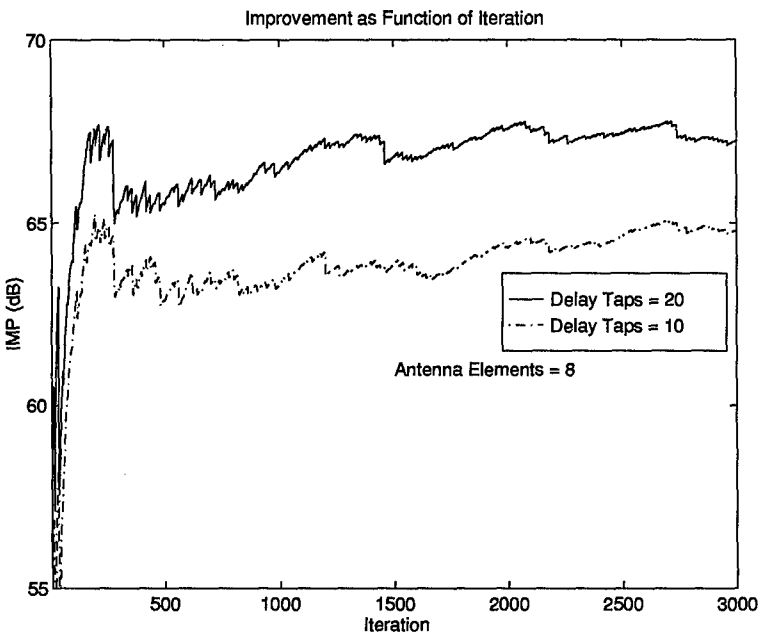

Figure 4.13 The Comparison Between $K = 10$ and $K = 20$ in the New Technique

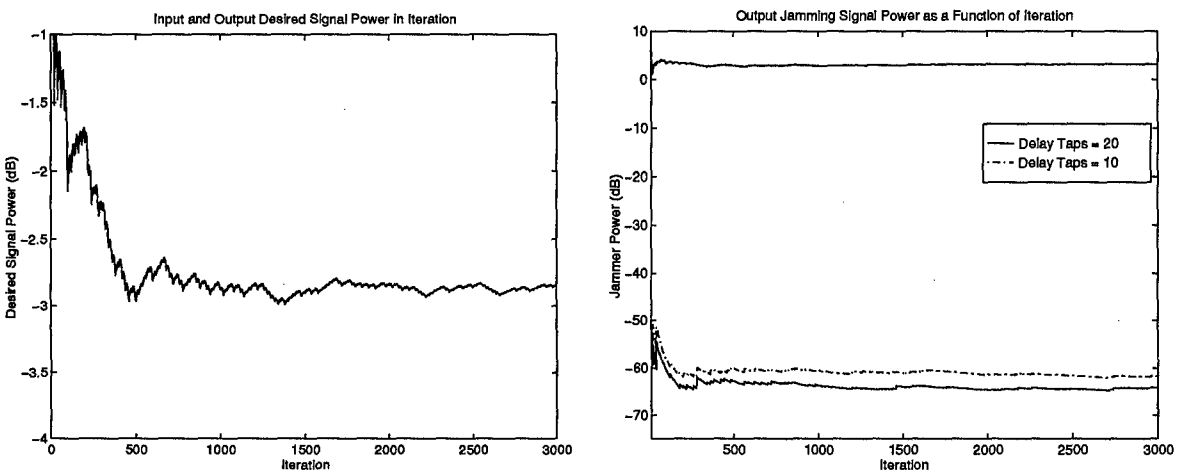

(a) (b)

Figure 4.14 The Comparison Between $K = 10$ and $K = 20$ in the New Technique (a) The Desired Signal Part, (b) the Jamming Signal Part

4.3 The Performance of a Spatial Smoothing Technique for Correlated Signals

This section presents an example case in which the desired signal and the jamming signal are correlated. The simulation uses the GSC adaptive weights, using the method which is described in section 3.4. Both signals have wide bandwidths, and the correlation coefficient between desired signal and jammer signal is 1,

$$\rho = \frac{\mathbf{R}_{sj}}{\mathbf{R}_s \mathbf{R}_j} = 1, \tag{4.28}$$

where $\mathbf{R}_{sj}$ is the cross correlation between the desired signal and the jamming signal and $\mathbf{R}_s$,$\mathbf{R}_j$ are the autocorrelation of the desired signal, the jamming signal respectively.

For this experiment, the LCMV beamformer with the TDL antenna array is used as in the previous section. The input signals and the weight vectors are the same as in Section 4.1. The only difference from section 4.1 is that the signals are correlated with each other.

The correlation matrix used for updating the weights is, as in Eq. 3.66,

$$\hat{\mathbf{R}} = \frac{1}{K} \sum_{k=1}^{K} \mathbf{R}_k. \tag{4.29}$$

The sub-array size M was fixed at 4 and the number of delayed taps is 10. The number of smoothing steps K is 5. The desired signal input power and the jamming signal input power are equal. Fig. 4.15 shows the SJR of three different cases as a function of iterations . The solid line shows the SJR_o when the signals are uncorrelated, while the dashed line and the dot-and-dashed line show the correlated signals case. The dashed line displays before decorrelation, which means $K = 1$. At that time, the SJR_o is reduced significantly, because the antenna can't put a null to the direction of the jamming signal as shown in Fig. 4.16(c). The jamming signal is a replica of the desired signal. The antenna array accepts the jamming signal as the desired signal. This fact shows that the adaptive antenna array is useless in the case of smart jammers and multipath signals because those jamming signals and multipath signals are highly correlated

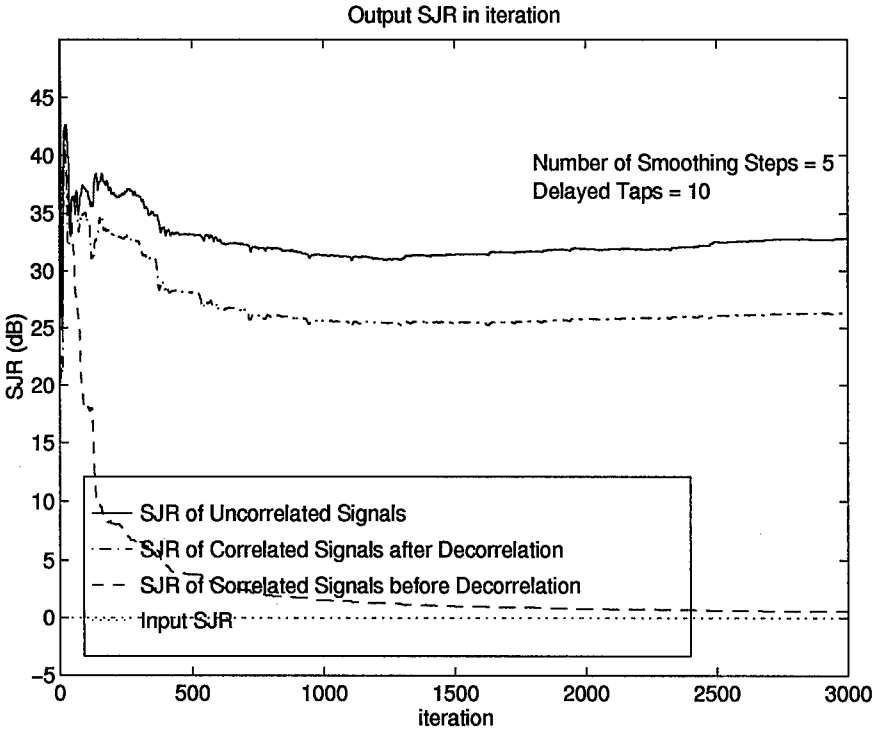

Figure 4.15 The Comparison of SJR After Performing the Spatial Smoothing Technique in the Presence of Correlated Signals

with the desired signal. However, after performing the smoothing technique to reduce the cross-correlation between the desired signal and jammer signal, the performance of adaptive antenna array improved significantly as shown in Fig. 4.15 by the lines as much as 20dB.

The desired signal power variation is shown in Fig. 4.16(a) as a function of iteration. As explained earlier, the desired signal has some distortion. The output power of the desired signal before decorrelation has a higher value than even the uncorrelated case. This occurs because some of the jamming signal is added to the desired signal. The jamming signal output power (J_o) before decorrelation signal is close to the jammer input power (J_i) (Fig. 4.16(b)), which shows no suppression at all in the jamming signal (Fig. 4.16(c)). After performing the smoothing technique however, the jamming signal output power is reduced, which shows the smoothing technique works for suppression of the jamming signal in the adaptive antenna array. Fig 4.16(d) shows the frequency characteristics after performing the spatial smoothing technique.

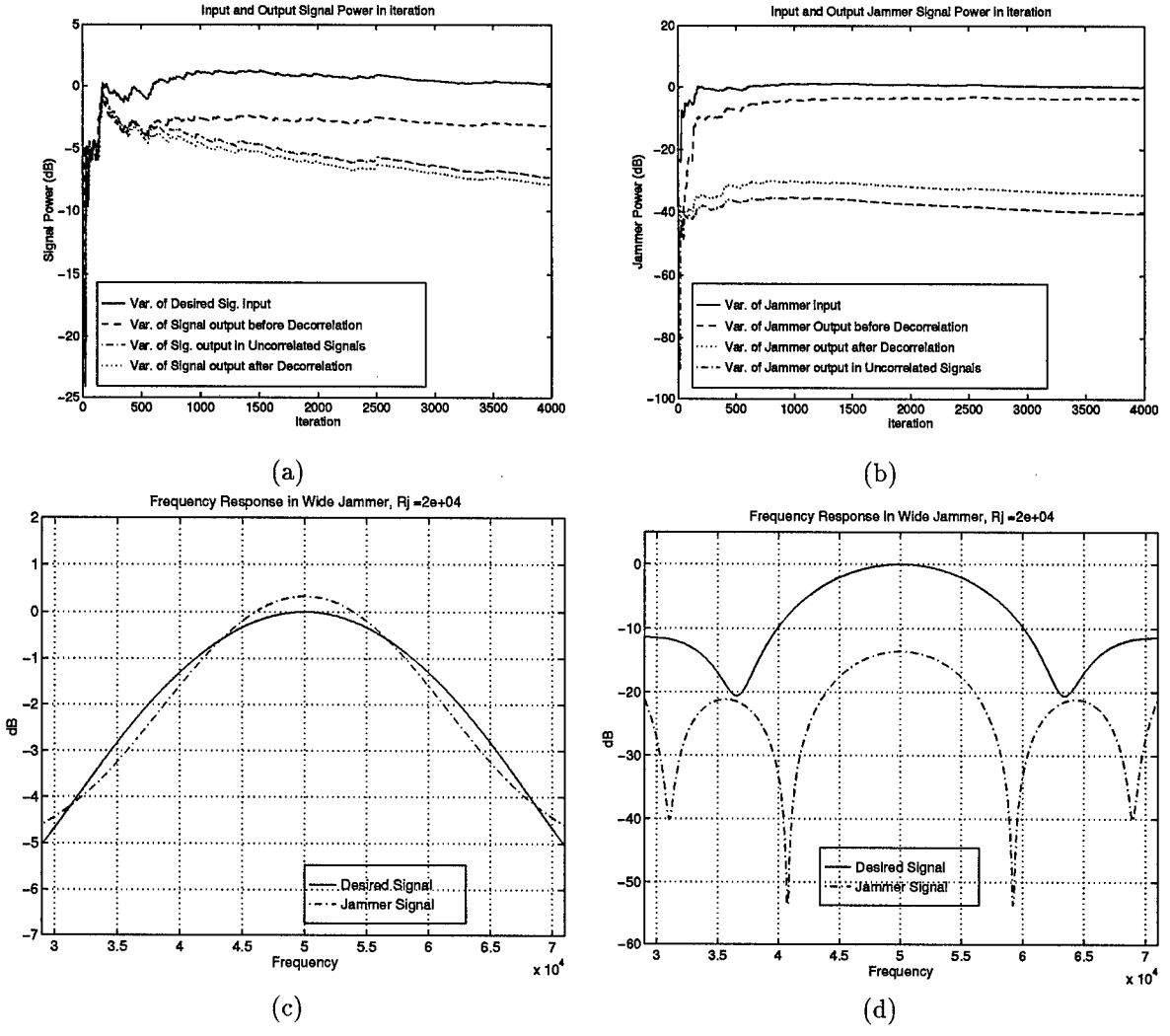

Figure 4.16 (a) The Desired Signal Power Variation, (b) The Jamming Signal Power Variation, (c) and (d) Frequency Characteristics Before Decorrelation and After Decorrelation, Respectively

4.4 Adaptive Filter for Narrowband Interference Suppression

The desired signal used here is the same as that which is generated in Section 4.1. The desired signal is assumed to be known in the receiver. The jamming signal is a single tone jammer. The number of taps is 12. The input signal vector, **u** and weight vector **w** are,

$$\begin{aligned} \mathbf{u} &= [u(n), u(n-1).....u(n-M+1)]^T \\ \mathbf{w} &= [w_1, w_2.....w_M]^T, \end{aligned}$$

where $M = 12$ is the number of taps.

The instantaneous estimated value of the tap-weight vector at time $n+1$ is computed by using the simple recursive relation as in Eq. 3.11,

$$\hat{\mathbf{w}}(n+1) = \hat{\mathbf{w}}(n) + \mu \mathbf{u}(n)[d^*(n) - \mathbf{u}^H(n)\hat{\mathbf{w}}]. \tag{4.30}$$

where $d(n)$ is the desired signal, and $\mu = \frac{0.5}{\lambda_{max}}$, is the step size parameter. λ_{max} is the largest eigenvalue of correlation matrix **R**.

The performance of this adaptive filter is demonstrated by exploring the SJR improvement. Fig. 4.17(a) shows the SJR improvement as a function of iterations. Fig. 4.17(b) shows the frequency characteristics of the adaptive filter. This system inserts the notch filter at the jammer carrier frequency at the cost suppressing that frequency in the desired signal. Therefore this system only works for narrowband jamming signal suppression. The jamming signal is suppressed well after just a few first iterations [Fig. 4.17(d)]. On the other hand, the desired signal is also suppressed at the first iterations. However as the number of iterations increases, the desired signal recovers its input power [Fig. 4.17(c)]. This means the notch filter is narrowing in order to avoid suppressing the desired signal. Eventually, the desired signal output power approaches the input power. Thus the SJR improvement of this system reaches the amount of jamming signal suppression.

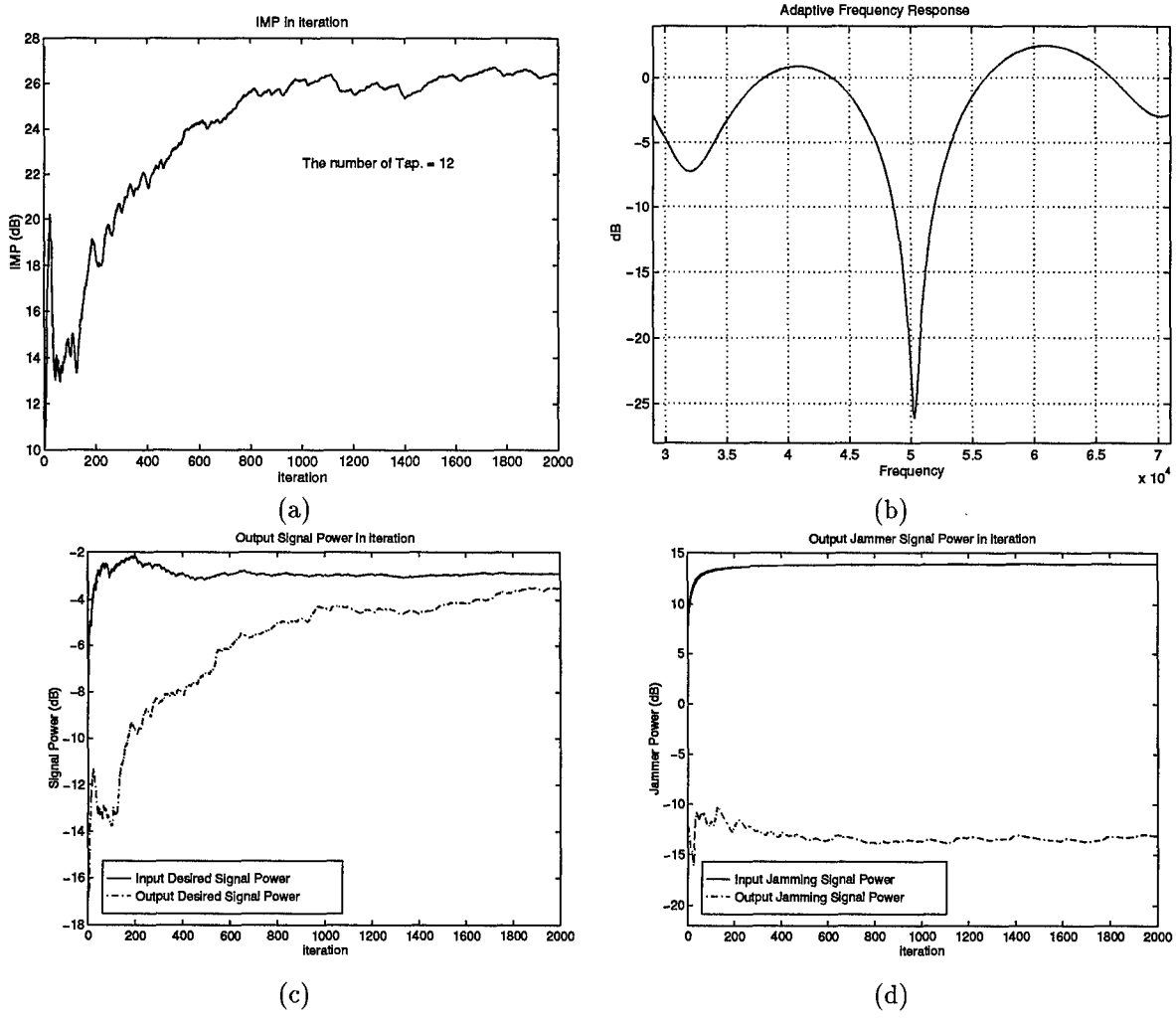

Figure 4.17 (a) Improvement of Adaptive Filter, (b) Frequency Characteristics of Adaptive Filter, (c) S_i and S_o, (d) J_i and J_o

4.5 Conclusion

This chapter considered the simulation of jamming signal suppression. The TDL antenna array is more effective than the LAS antenna array to suppress the wideband interference in the LCMV-GSC beamformer. In the frequency-hopped environment, a new technique, which the hopping frequencies are used in the desired signal direction gain-only constraint matrix, suppressed wideband jamming signal more efficiently than the conventional method. The smoothing technique was demonstrated to reduce the cross-correlation of the desired and jamming signal. After performing this technique, the jamming signal was suppressed significantly. Finally, the performance of the adaptive filter was shown for suppression of the narrowband jamming signal. The next chapter will conclude this research and recommend research topics for future study.

V. Conclusion and Recommendations for Future Research

5.1 Conclusion

Interference(s) is a significant problem in military communication operations. This thesis examined the suppression of interference using the SJR as a metric for comparing the adaptive temporal filter and adaptive spatial filter (i.e. adaptive beamforming). In these systems, the optimum weights are selected to optimize the response based on the statistics of the data. The data statistics are often unknown and may change with time so adaptive algorithms are used to obtain weights that converge to the statistically optimum solution. Here, the most well-known and simple algorithm, LMS algorithm was used.

For the class of beamformer, a procedure was presented for the design and implementation of a LCMV beamformer for wideband interference suppression. This beamformer attempts to achieve the minimum output variance subject to the constraint on the gain in the desired signal direction. The structure used extends the GSC to implement and to analyze the LCMV beamformer. The GSC separates the weight vector with constrained and unconstrained components. The constrained components represent the gain and phase of the desired signal and its direction. The unconstrained components are adjusted using the LMS adaptive algorithm. Using the LCMV-GSC beamformer, it was shown that the TDL adaptive antenna array is more effective for the suppression of wideband jammer suppression than the LAS adaptive antenna array.

Further, in the frequency-hopped environment, the new technique was introduced which used each hopping frequency for the desired signal direction gain-only constraint in the LCMV beamformer. This new technique improved the capability of wideband interference suppression over the conventional technique which used only the center frequency in the constraint matrix. The reason is that the new technique does not distort the desired signal, while the conventional technique severely distorts the desired signal.

Then the effect of the spatial smoothing in the presence of the correlated signals was ana-

lyzed. When the desired signal was correlated with the jamming signal, the LCMV beamforming performed poorly because the adaptive antenna array accepted the jamming signal as the desired signal. Therefore it couldn't put a null in the direction of the jamming signal. After performing the spatial smoothing technique, however, the adaptive antenna array inserted a deep null for suppression of the jamming signal.

Finally, the adaptive temporal filter was shown to adequately suppress narrowband jammers. The drawback of this system however, is that it can not be used to suppress wideband interference.

5.2 Recommendation for Future Study

There are three main areas of research that can be derived from this thesis effort. These three areas are,

- Adaptive Beamforming for Wideband Interference.
- Spatial Smoothing in the Presence of Correlated Signals.
- Adaptive Filter for Narrowband Interference.

In the first of these areas, there are the desired signal distortions when using the conventional technique. Future study is recommended to investigate a way to decrease this distortion. Since the desired signal is distorted, the SJR_o decreases even though the number of delayed taps increases. Thus it is recommended to study the optimum number of delayed taps and antenna elements. This thesis was limited to a single jammer and jamming signal direction. The performance of interference suppression needs to be observed for a larger number of jammers and for changing directions. Because of the computational consideration, the partially adaptive beamformer with array composed of large numbers of sensors has been investigated and remained as a good topic.

Another area for possible research is suppression of the jamming signal correlated with the desired signal. This area arises due to multipath propagation or smart jamming and creates a serious problem for conventional adaptive beamformer. The spatial smoothing technique is based

on averaging to destroy the correlation between the signal and interference. However, correlated interference suppression still remains an important research topic.

A final recommended area for future research regards temporal adaptive filters. It is recommended to compare the performance of interference suppression of the time domain adaptive filter with the transform domain adaptive filter and the transform domain excisor.

Appendix A. Constrained Optimization

The typical constraints optimization problem has the form

$$\min_{\mathbf{x}} f(\mathbf{x}), \quad \textit{subject to} \quad \mathbf{g}(\mathbf{x}) = \mathbf{0}, \tag{A.1}$$

where f(·) is the scalar-valued objective function and $\mathbf{g}(\cdot)$ is the vector-valued *constaint function.* The classical approach to solving a constrained optimization problem is the method of *Lagrange multipliers*, λ. The *Lagrangian* of a constrained optimization problem is defined to be the scalar-valued function

$$L(\mathbf{x}, \lambda) = f(\mathbf{x}) + \lambda \mathbf{g}(\mathbf{x}). \tag{A.2}$$

In the case at hand one minimize $\mathbf{w}^H \mathbf{R}_x \mathbf{w}$ subject to the linear constraint $\mathbf{C}^H \mathbf{w} = \mathbf{f}$. $\mathbf{w}$ is weight vector and $\mathbf{R}_x$ is autocorrelation vector of input vector, $\mathbf{x}$. The constraint $g(\mathbf{x}) = \mathbf{C}^H \mathbf{w} - \mathbf{f}$ is a scalar-valued one where $\mathbf{C}$ is the constraint matrix and $\mathbf{f}$ is response vector. The Lagrangian is

$$L(\mathbf{w}, \lambda) = \mathbf{w}^H \mathbf{R}_x \mathbf{w} + \lambda(\mathbf{C}^H \mathbf{w} - \mathbf{f}). \tag{A.3}$$

Its gradient is $2\mathbf{R}\mathbf{w} + \lambda \mathbf{C}$ with a solution,

$$\mathbf{w}_{opt} = -\lambda_{opt} \mathbf{R}^{-1} \frac{\mathbf{C}}{\mathbf{2}}. \tag{A.4}$$

To find the value of the Lagrange multiplier, this solution must satisfy the constraint. Imposing the constraint,

$$\lambda_{opt} \mathbf{C}^H \mathbf{R}^{-1} \mathbf{C} = -2\mathbf{f}. \tag{A.5}$$

By solving with λ_{opt},

$$\lambda_{opt} = -\frac{2\mathbf{f}}{\mathbf{C}^H \mathbf{R}^{-1} \mathbf{C}} \tag{A.6}$$

The total solution is

$$\mathbf{w}_{opt} = \frac{\mathbf{fR}^{-1}\mathbf{C}}{\mathbf{C}^{H}\mathbf{R}^{-1}\mathbf{C}} \tag{A.7}$$

Appendix B. Matlab Coding

B.1 Generation of the Signals

```
Rs = $2*10^5$;        % The sampling frequency.
f1 = 50000;           % The carrier frequency of the desired signal.
f2 = 50000;           % The carrier frequency of the jamming signal.
N = 5000;             % The number of samples.
```

B.1.1 General Wideband Signals.

```
x=randn(1,N);                                  % Generate the random noise
fcut11=(Rc)/Rs*2;                              % Cut frequency of the filter.
[n,wn]=cheb2ord(fcut11,fcut11+0.02,0.05,60);   % Decide order of the filter.
[B,A]=cheby2(n,60,wn);                         % Decide the filter coefficient.
signal=filter(B,A,x);                          % Filters the data by B and A.
for i=1:N
   expon(i,1)=cos(2*pi*f1/Rs*(i-1));           % Carrier frequency
end
signal=signal*expon;
```

B.1.2 Frequency Hopping Signals.

```
% Generate R bits bipolar data sequence having P data rate.
bi = sign(randn(1,R));
data = bi'*ones(1,P);
datasequence = reshape(data',1,P*R);


% Generate BFSK signal of R bits.
```

```
bfsk=zeros(M,length(n));        % Initial value of BFSK signal.
w1=1000;                        % The first frequency of BFSK signal.
w2=2000;                        % The second frequency of BFSK signal.
n=1:20;
bfsk1=cos(2*pi*w1.*n./fsim);    % The data sequence of the first BFSK signal.
bfsk2=cos(2*pi*w2/fsim.*n);     % The data sequence of the second BFSK signal.
for i=1:R                       % Decide the bipolar data sequence
  if bi(i)==1                   % using BFSK sequences.
     bfsk(i,:)=bfsk1;
  else
     bfsk(i,:)=bfsk2;
  end
end
databfsk=reshape(bfsk',1,M*length(n)); % Generate the BFSK signal.
% Generate hopping signal.
  h=zeros(pg,N);                        % Initial value of hopping signal.
  for i=1:pg
    num(i)=round(rand(1,1)*pg);
  end
  for i=1:pg;
   ff1(i)=fh*num(i)+fi;                 % Decide the hopping frequency.
     for n=1:N;
      h(i,n)=cos(2*pi*ff1(i)*n/fsim);   % Make the hopping sequence.
     end
  end
  h=reshape(h',1,N*pg);
```

```
% Generate the FH (Frequency Hopping) signal.
  signal=databfsk.*h;
```

B.2 LCMV Adaptive Beamforming

```
  M = 12;                              % The number of antenna elements.
  K = 5;                               % The number of delayed Taps.
  mu1 = 0.0002;                        % The step size parameter.
  thd = 30*pi/180;                     % The desired signal direction.
  thi = -30*pi/180;                    % The jamming signal direction.
  Td = 2/f1*sin(thd);                  % Propagation delay by signal.
  Ti = 2/f1*sin(thi);                  % Propagation delay by jammer.
  ff1                                  % The signal hopping frequency.

% Generate the constraint matrix for the LMS adaptive array antenna.
  for ii=1:M
    d(ii,1)=exp(-sqrt(-1)*2*pi*(fc)/2/(fc)*sin(thd)*(ii-1));
  end
  C=d;                 % Constraint matrix for desired direction gain-only.
  g=1;                 % The response of the beamformer.
  Wq=C*inv(C'*C)*g;    % Wq is the quiescent weight vector.

% The blocking Matrix.
  [m,n] = size(C);
  C = zeros(m,m);
  [Q,R] = qr(C);
  Ca = Q(:,n+1:m);     % The blocking matrix.
```

```
% Generate the constraint matrix for the TDL adaptive array antenna.
  for j=1:K
    for ii=1:M
      d(ii,1)=exp(-sqrt(-1)*2*pi*(fc)/2/(fc)*sin(thd)*(ii-1)); % Array response
    end                                                        % vector.
      C(:,j)=[zeros(M*(j-1),1); d; zeros(M*(K-j),1)];          % Constraint
  end                                                          % matrix
  f=[1 zeros(1,K-1)]';              % The response of the beamformer.
  Wq=C*inv(C'*C)*g;                 % Wq is the quiescent weight vector.
  [Ca]=block(C);                    % Blocking Matrix

% The LMS antenna input signal vector and LMS algorithm.
 si=0;
 for i=N1:N
   si=si+1
   for j=1:M
     ud(j,si)=inputd(i-Td*Rs*(j-1));
     ui(j,si)=winputi(i-Ti*Rs*(j-1));
   end
   u(:,si)=(ud(:,si)+ui(:,si));             % The input signal vector.
   R=u(:,si)*u(:,si)';                      % Correlation of the input vector.
   Rx=Ca'*R*Ca;
   px=Ca'*R*Wq;
   wa(:,si+1)=wa(:,si)+mu*(px-Rx*wa(:,si)); % Unconstrained component in GSC.
   W(:,si)=Wq-Ca*wa(:,si);                  % The LMS weight estimate.
```

```
 end


% The TDL antenna input signal vector and optimum weights value.
   si=0;
  for i=N1:N
    si=si+1
    for n=1:K
     for j=1:M
       ud(j+(n-1)*M,si)=inputd(i-Td*Rs*(j-1)-(n-1));
       ui(j+(n-1)*M,si)=winputi(i-Ti*Rs*(j-1)-(n-1));
     end
    end
  end
  u=ud+ui;                        % The input signal vector.
  R=u*u'/(N-N1)                   % Correlation of the input vector.
  wa=inv(Ca'*R*Ca)*Ca'*R*Wq;      % Unconstrained component weights in GSC.
  Wopt=Wq-Ca*wa;                  % Optimum weight of the LCMV-GSC beamformer.


% The new model for constraint matrix, input vector, and LMS weight estimate\\
% in the frequency hopped environment.
  si=0;
 for i=1:N
  for j=1:K
    for ii=1:M
      d(ii,1)=exp(-sqrt(-1)*2*pi*ff1(i)/2/(f1)*sin(thd)*(ii-1));  % Array response
    end                                                           % vector.
```

```
    C(:,j)=[zeros(M*(j-1),1); d; zeros(M*(K-j),1)];          % The constraint
 end                                                          % matrix
 f=[1 zeros(1,K-1)]';              % The response of the beamformer.
 Wq=C*inv(C'*C)*g;                 % Wq is the quiescent weight vector.
 [Ca]=block(C);                    % Blocking Matrix
for n=1:K
 for j=1:M
   ud(j+(n-1)*M,i)=inputd(i)*exp(-sqrt(-1)*2*pi*ff1(i)*(j-1)/2/(f1)\\
                  *sin(thd))*exp(-sqrt(-1)*2*pi*To*(ff(i))*(n-1));
   ui(j+(n-1)*M,i)=winputi(i)*exp(-sqrt(-1)*2*pi*ff2(i)*(j-1)/2/(f1)\\
                  *sin(thi))*exp(-sqrt(-1)*2*pi*To*(ff2(i))*(n-1));
 end
end
  u(:,si)=(ud(:,si)+ui(:,si));             % The input signal vector.
  R=u(:,si)*u(:,si)';                      % Correlation of the input vector.
  Rx=Ca'*R*Ca;
  px=Ca'*R*Wq;
  wa(:,si+1)=wa(:,si)+mu*(px-Rx*wa(:,si)); % Unconstrained component in GSC.
  W(:,si)=Wq-Ca*wa(:,si);                  % The LMS weight estimate.
 end
```

B.3 Spatial Smoothing Technique

```
% Add the decorrelation factor in the LCMV-GSC beamformer.
 R=zeros(M*K);                            % Initial value of correlation.
 si=0;
 for i=N1:N
```

```
K1 = 5;                                    % The smoothing steps
for MN=1:K1
 for j=1:K
   ti=0;
   for ii=MN:M+Mn-1
     ti=ti+1;
     d(ti,1)=exp(-sqrt(-1)*2*pi*f1/2/(f1)*sin(thd)*(ii-1));
   end
     C(:,j)=[zeros(M*(j-1),1); d; zeros(M*(K-j),1)];          % The constraint
 end                                                          % matrix
 f=[1 zeros(1,K-1)]';              % The response of the beamformer.
 Wq=C*inv(C'*C)*g;                 % Wq is the quiescent weight vector.
 [Ca]=block(C);                    % Blocking Matrix
  for n=1:K
   tt=0;
   for j=MN:M+MN-1
     tt=tt+1;
     ud(tt+(n-1)*M,si)=inputd(i-Td*Rs*(j-1)-(n-1));
     ui(tt+(n-1)*M,si)=winputi(i-Ti*Rs*(j-1)-(n-1));
   end
  end
 u(:,si)=(ud(:,si)+ui(:,si));              % The input signal vector.
 R=R+u(:,si)*u(:,si)';                     % Correlation of the input vector.
end
 R=R/K;
 Rx=Ca'*R*Ca;
```

```
  px=Ca'*R*Wq;
  wa(:,si+1)=wa(:,si)+mu*(px-Rx*wa(:,si));  % Unconstrained component in GSC.
  W(:,si)=Wq-Ca*wa(:,si);                   % The LMS weight estimate.
end
```

B.4 Adaptive Filter

```
 inputd=[zeros(1,M-1) inputd];              % Put a leading 0 in x
 inputi=[zeros(1,M-1) inputi];
 input=[zeros(1,M-1) input];
 w=zeros(M,N+1);                            % Clear tap weights
 y=zeros(1,N);                              % Observed output
 e=zeros(1,N);                              % Output error
 for n=1:N-M
  for j=1:M
     u(j,n)=input(n+M-j);                   % Input vector
  end
  y(n) = w(:,n)'*u(:,n);                    % Output point
  e(n) = inputd(n+M-1)-y(n);                % Error
  w(:,n+1) = w(:,n) + mu*u(:,n)*e(n)';      % Filter weights
 end
```

Bibliography

1. Bakhru, K. and D. Torrieri (1984), "The Maximin Algorithm for Adaptive Arrays and Frequency Hopped Communication," *IEEE Trans. on Antennas and Propagation*, vol. AP-32, no. 9, pp. 919-928, Sep. 1984.
2. Buckley, M. Kevin and Lloyd J. Griffiths (1986), "An Adaptive Generalized Sidelobe Canceller with Derivative Constraints," *IEEE Trans. on Antennas and Propagation*, vol. AP-34, No. 3, March 1986.
3. Capon, J. (1969) "High-Resolution frequency-wavenumber spectrum analysis," *Proc. IEEE*, vol. 57, pp. 1408-1418.
4. Compton, R. T. (1985) "The Performance of an LMS Adaptive Array with Frequency Hopped Signals," *IEEE Trans. on Aerospace and Electronic Systems,* vol. AES-32, no. 9, pp. 360-371, Jan. 1988.
5. Compton, R. T. (1988) "The bandwidth performance of a two-element adaptive array with tapped delay-line processing," *IEEE Trans. on Antennas and Propagation,* vol. 36, no. 1, pp. 5-14, Jan. 1988.
6. Compton, R. T. (1988) "The relationship between tapped delay line and FFT processing in Adaptive arrays," *IEEE Trans. on Antennas and Propagation,* vol. 36, no. 1, pp. 15-26, Jan. 1988.
7. Davidovici, Sorin and Emmanuel G. Kanterakis, (1989) Narrowband interference rejection using real-time Fourier Transforms, *IEEE Trans. on Comm.,* vol. 37, no. 7, pp. 713-722, July 1989.
8. Frost, O. (1972) "An algorithm for linearly constrained adaptive array processing," *Proc. IEEE,* vol. 60, 1972.
9. Gevargiz, J., Milstein, Laurence B., and P. K. Das *Adaptive narrowband interference rejection in a DSSS intercept receiver using transform domain signal processing techniques*, IEEE Trans. on Comm. vol. 37, no. 12, pp. 1359-1366, Dec. 1989.
10. Godard, D. N. (1974) "Channel equalization using a Kalman filter for fast data transmission," *IBM K. Res. Dev.*, vol. 18, pp. 267-273.
11. Griffiths, L. J. and C. W. Jim, (1982) "An alternative approach to linearly constrained adaptive beamforming," *IEEE Trans. on Antennas and Propagation,* vol. 30, Jan. 1982.
12. Haykin, S., and Allan Steinhardt, (1992) *Adatptive Radar Detective and Estimation* Wiley Series in Remote Sensing, chapter 4, New York.
13. Howells, P.W. (1976). "Explorations in fixed and adaptive resolution at GE and SURC," *IEEE Trans. on Antennas and Propagation,* vol. AP-24, Special Issue on Adpative Antennas, pp. 575-584.
14. Hsu, F. M. and Arthur A, Giordano, (1978) "Digital Whitening Techniques for Improving Spread Spectrum Communications Performance in the presence of Narrowband Jamming and Interference," *IEEE Trans. on Comm.* vol. COM-26, no. 2, pp. 209-216, Feb. 1978.
15. Ketchum, John W. and John G. Proakis (1982) "Adaptive Algorithms for Estimating and suppressing narrowband interference in PN SS systems," *IEEE Trans. on Comm.,* vol. COM-32, no, 5, pp. 913-928, May 1982.
16. Levinson, N. (1947). "The Wiener RMS error criterion in filter design and prediction," *J. Math Phys.*, vol. 25, pp. 261-278

17. Mayhan, J. T., A. J. Simmons and W. C. Summings, (1981) "Wideband adaptive antenna nulling using tapped delay-lines," *IEEE Trans. on Antennas and Propagation,* vol. AP-20, no. 6, pp. 923-936, Nov. 1981.

18. Mikulanicz, George S., (1990) *Performance of an Acoustic Charge Transport (ACT) Programable Tapped delay line (PTDL) fo signal processing Applications.* MS Thesis, AFIT/GE/EE90D-40. School of Engineering, Air Force Institute of Technology, Wright-Patterson AFB OH, DEC. 1990.

19. Milstein, Laurence B. and P. K. Das (1980) "An analysis of a real time transform domain filtering digital comm. system–Part I: Narrowband interference rejection," *IEEE Trans. on Comm.,* vol. COM-28, no. 6, pp. 816-824, June 1980.

20. Milstein, Laurence B. (1988) "Interference Rejection Techniques in Spread Spectrum Communication," *Proc. of the IEEE,* vol. 76, no. 6, pp. 657-671, June 1988.

21. Najar, M., and M. A. Lagunas (1995) "High Resolution Adpative Arrays Based on Random Processing Techniques : Frequency Hopping Modulation," *IEEE ISACS* pp. 1737-1740,

22. Nordholm, S., I. Claesson, and P. Eriksson, (1992) "The Broadband Wiener solution for Griffiths-Jim beamformers," *IEEE Trans. on Signal Processing,* vol. 40, no. 2, Feb. 1992.

23. Peterson, L. R., Ziemer, E. R. and D. E. Borth (1995) *Introduction to Spread Spectrum Communications*, Prentice Hall Englewood Cliffs, NJ.

24. Plackett, R. L. (1950). "Some theorems in least squares," *Biometrika*, Vol. 37, p.149.

25. Reddy, V. U., A. Paulraj, and T. Kailath (1987), "Performance Analysis of the Optimum Beamformer in the Presence of Correlated Sources and its Behavior Under Spatial Smoothing," *IEEE Trans. on Acoustics Speech and Signal Processing,* vol. ASSP-35, pp. 927-936, July, 1987.

26. Reed, Francis A. and Paul L. Feintuch (1981) "A comparison of LMS adaptive cancellers implemented in the Frequency domain and the Time domain," *IEEE Trans. on Acoustics Speech and Signal Processing,* vol. ASSP-29, No. 3, pp. 770-775, June 1981.

27. Rodgers, W. E. and R. T. Compton, Jr., (1979) "Adaptive array bandwidth with tapped delay-line processing," *IEEE Trans. on Aerspace and Electronic Systems,* vol. AES-15, no. 1, pp. 21-27, Jan. 1979.

28. Saulnier, Gary J., P. K. Das, and Laurence B. Milstein, (1984) "Suppression of narrowband interference rejection techniques in DSSS systems," *IEEE Trans. on Comm.,* vol. COM-32, no. 11, pp. 1227-1232, Nov. 1984.

29. Saulnier, Gary J., P. K. Das, and Laurence B. Milstein, (1985) "An adaptive digital suppression filter for DSSS communications," *IEEE Journal on Selective Areas in Comm.,* vol. SAC-3, no. 5, pp. 676-685, Sep. 1985.

30. Saulnier, Gary J. (1990) "Interference suppression using a SAW-based adaptive filter," *IEEE MILCOM '90*, Monterey, CA, Sep30-Oct 3, 1990, pp. 970-974.

31. Saulnier, Gary J. (1992) "Supperssion of narrowband jammers in a SS receiver using transform domain adaptive filtering," *IEEE J. on Sel. Areas in Comm.,* vol. SAC-10, No. 4, pp. 742-749, May 1992.

32. Shephard, Michael M. (1982) *The performance of a PN SS Receiver preceded by an adaptive interference suppression filter*, MS Thesis, AFIT/GE/EE/82-62. School of Engineering, Air Force Institute of Technology, Wright-Patterson AFB OH, DEC. 1982.

33. Skolnik, M. I. (1982), *Introduction to Radar Systems*, Second Edition, McGraw-Hill, New York.

34. Torrieri, D. and K. Bakhru (1987), "Frequency Compensation in an Adaptive Antenna System for Frequency Hopping Frequency," *IEEE Trans. on Aerospace and Electronic Systems,* vol. AES-23, no. 4, pp. 448-467, July 1987.

35. Wang, Hefeng, Ryuji Kohno, and Hideki Imai (1993) "Adaptive Array Antenna Combined with Tapped Delay Line Using Processing Gain for Direct Sequence/Spread Spectrum Multiple Access System," *Electronics and Communications in Japan,* Part 1, Vol. 76, No. 5, 1993.

36. Way, John R. (1984) *The performance of a new adaptive filter for digital communications,* MS Thesis, AFIT/GE/EE84s-12, School of Engineering, Air Force Institute of Technology, Wright-Patterson AFB OH, June 1984.

37. White, W. D. (1983) "Wideband interference cancelllation in adatptive sidelobe cancellers," *IEEE Trans. on Aerospace and Electronic System,* vol. 19, no. 6, pp. 915-925, Nov. 1983.

38. Widrow, B., P. E. Mantey, L. J. Griffiths, and B. B. Goode, (1967) "Adaptive antenna systems," *Proc. IEEE,* vol. 55, no. 12, pp. 2143-2159, Dec. 1967.

39. Widrow, B. (1970). "Adaptive filters," in *Aspects of Network and System Theory,* ed. R. E. Kalman and N. DeClaris, Holt, Rinehart and Winston, New York.

40. Widrow, B., K. M. Duvall, R. P. Gooch, and W. C. Newman (1982), "Signal Cancellation Phenomena in Adaptive Antennas: Causes and Cures," *IEEE Trans. on Antennas and Propagation,* vol. AP-30 pp. 469-478, May, 1982.

41. Widrow, B. and S. D. Stearns (1985), *Adaptive Signal Processing* Prentice Hall, Englewood Cliffs, NJ.

42. Wiener, N., and E. Hopf (1931). "On a class of singular integral equations," *Proc. Prussian Acad. Math Phys. Ser.,* p.696.

Vita

Wonjin Park [redacted] He completed high school at ScoKang High School in Kwangju, Korea. In 1988, Wonjin attended the Korean Military Academy (KMA). In April 1992, he graduated KMA with a Bachelor of Science Degree in Electrical Engineering and was commissioned a Second Lieutenant in the Republic of Korean Army (ROKA). He was then assigned as a Platoon Leader to 7 Division Reconnaissance company. In 1994, Wonjin was sponsored by the ROKA to complete a Master of Science Degree in Electrical Engineering at the Air Force Institute of Technology, Dayton, OH.

[redacted]

REPORT DOCUMENTATION PAGE

Form Approved
OMB No. 0704-0188

1. AGENCY USE ONLY *(Leave blank)*	2. REPORT DATE	3. REPORT TYPE AND DATES COVERED
	December 1996	Master's Thesis

4. TITLE AND SUBTITLE
Interference Suppression for Spread Spectrum Signals
Using Adaptive Beamforming and Adaptive Temporal Filter

5. FUNDING NUMBERS

6. AUTHOR(S)
Wonjin Park

7. PERFORMING ORGANIZATION NAME(S) AND ADDRESS(ES)
Air Force Institute of Technology, WPAFB OH 45433-6583

8. PERFORMING ORGANIZATION REPORT NUMBER
AFIT/GE/ENG/96D-14

9. SPONSORING/MONITORING AGENCY NAME(S) AND ADDRESS(ES)
Lawrence L. Gutman
WL/AAMI

10. SPONSORING/MONITORING AGENCY REPORT NUMBER

11. SUPPLEMENTARY NOTES

12a. DISTRIBUTION/AVAILABILITY STATEMENT
Approved for Public release; Distribution Unlimited

12b. DISTRIBUTION CODE

13. ABSTRACT *(Maximum 200 words)*

Interference and jamming signals are a serious concern in an operational military communication environment. This thesis examines the utility and performance of combining adaptive temporal filtering with adaptive spatial filtering (i.e. adaptive beamforming) to improve the signal-to-jammer ratio (SJR) in the presence of narrowband and wideband interference. Adaptive temporal filters are used for narrowband interference suppression while adaptive beamforming is used to suppress wideband interference signals. A procedure is presented for the design and implementation of a linear constraints minimum variance generalized sidelobe canceler (LCMV-GSC) beamformer. The adaptive beamformer processes the desired signal with unity gain while simultaneously and adaptively minimizing the output due to any undesired signal. Using the LCMV-GSC beamformer with a least mean squares (LMS) adaptive algorithm, it was shown that the tapped delay line (TDL) adaptive antenna array is more effective for the suppression of wideband jammer suppression than the linear array sensors (LAS) adaptive antenna array. Also a new technique for adaptive beamforming is presented which improves wideband interference suppression in a frequency-hopped environment. The output SJR improvement for the new technique compared to the conventional technique is as much as 15dB. Sometimes, multipath signals and jammers generated by a smart enemy are correlated with the desired signal which destroys the traditional beamformer's performance. After performing a spatial smoothing technique, adaptive beamforming can also be effective in suppressing the jamming signals that are highly correlated with the desired signal.

14. SUBJECT TERMS	15. NUMBER OF PAGES
Adaptive Beamforming, Frequency Hopping, Adaptive Temporal Filter, LMS Adaptive Algorithm	97
	16. PRICE CODE

17. SECURITY CLASSIFICATION OF REPORT	18. SECURITY CLASSIFICATION OF THIS PAGE	19. SECURITY CLASSIFICATION OF ABSTRACT	20. LIMITATION OF ABSTRACT
UNCLASSIFIED	UNCLASSIFIED	UNCLASSIFIED	UL

GENERAL INSTRUCTIONS FOR COMPLETING SF 298

The Report Documentation Page (RDP) is used in announcing and cataloging reports. It is important that this information be consistent with the rest of the report, particularly the cover and title page. Instructions for filling in each block of the form follow. It is important to ***stay within the lines*** to meet ***optical scanning requirements***.

Block 1. Agency Use Only *(Leave blank)*.

Block 2. Report Date. Full publication date including day, month, and year, if available (e.g. 1 Jan 88). Must cite at least the year.

Block 3. Type of Report and Dates Covered. State whether report is interim, final, etc. If applicable, enter inclusive report dates (e.g. 10 Jun 87 - 30 Jun 88).

Block 4. Title and Subtitle. A title is taken from the part of the report that provides the most meaningful and complete information. When a report is prepared in more than one volume, repeat the primary title, add volume number, and include subtitle for the specific volume. On classified documents enter the title classification in parentheses.

Block 5. Funding Numbers. To include contract and grant numbers; may include program element number(s), project number(s), task number(s), and work unit number(s). Use the following labels:

C	- Contract	**PR**	- Project
G	- Grant	**TA**	- Task
PE	- Program Element	**WU**	- Work Unit Accession No.

Block 6. Author(s). Name(s) of person(s) responsible for writing the report, performing the research, or credited with the content of the report. If editor or compiler, this should follow the name(s).

Block 7. Performing Organization Name(s) and Address(es). Self-explanatory.

Block 8. Performing Organization Report Number. Enter the unique alphanumeric report number(s) assigned by the organization performing the report.

Block 9. Sponsoring/Monitoring Agency Name(s) and Address(es). Self-explanatory.

Block 10. Sponsoring/Monitoring Agency Report Number. *(If known)*

Block 11. Supplementary Notes. Enter information not included elsewhere such as: Prepared in cooperation with...; Trans. of...; To be published in.... When a report is revised, include a statement whether the new report supersedes or supplements the older report.

Block 12a. Distribution/Availability Statement. Denotes public availability or limitations. Cite any availability to the public. Enter additional limitations or special markings in all capitals (e.g. NOFORN, REL, ITAR).

- **DOD** - See DoDD 5230.24, "Distribution Statements on Technical Documents."
- **DOE** - See authorities.
- **NASA** - See Handbook NHB 2200.2.
- **NTIS** - Leave blank.

Block 12b. Distribution Code.

- **DOD** - Leave blank.
- **DOE** - Enter DOE distribution categories from the Standard Distribution for Unclassified Scientific and Technical Reports.
- **NASA** - Leave blank.
- **NTIS** - Leave blank.

Block 13. Abstract. Include a brief *(Maximum 200 words)* factual summary of the most significant information contained in the report.

Block 14. Subject Terms. Keywords or phrases identifying major subjects in the report.

Block 15. Number of Pages. Enter the total number of pages.

Block 16. Price Code. Enter appropriate price code *(NTIS only)*.

Blocks 17. - 19. Security Classifications. Self-explanatory. Enter U.S. Security Classification in accordance with U.S. Security Regulations (i.e., UNCLASSIFIED). If form contains classified information, stamp classification on the top and bottom of the page.

Block 20. Limitation of Abstract. This block must be completed to assign a limitation to the abstract. Enter either UL (unlimited) or SAR (same as report). An entry in this block is necessary if the abstract is to be limited. If blank, the abstract is assumed to be unlimited.